Mon. Not. R. Astron. Soc. **391,** 825–843 (2008) doi:10.1111/j.1365-2966.2008.13915.x

Formation and dynamical evolution of multiple stellar generations in globular clusters

Annibale D'Ercole,[1⋆] Enrico Vesperini,[2] Francesca D'Antona,[3] Stephen L. W. McMillan[2] and Simone Recchi[4,5]

[1]*INAF – Osservatorio Astronomico di Bologna, via Ranzani 1, I-40127 Bologna, Italy*
[2]*Department of Physics, Drexel University, Philadelphia, PA 19104, USA*
[3]*INAF – Osservatorio Astronomico di Roma, via di Frascati 33, I-00040 Monteporzio, Italy*
[4]*INAF – Osservatorio Astronomico Trieste, via G.B. Tiepolo 11, 34131 Trieste, Italy*
[5]*Institute of Astronomy, Vienna University, Türkenschanzstrasse 17, A-1180 Vienna, Austria*

Accepted 2008 September 4. Received 2008 September 2; in original form 2008 July 12

ABSTRACT

We study the formation and dynamical evolution of clusters with multiple stellar generations. Observational studies have found that some globular clusters host a population of second generation (SG) stars which show chemical anomalies and must have formed from gas containing matter processed in the envelopes of first generation (FG) cluster stars. We study the SG formation process by means of one-dimensional (1D) hydrodynamical simulations, starting from a FG already in place and assuming that the SG is formed by the gas ejected by the asymptotic giant branch (AGB) stars. This gas collects in a cooling flow into the cluster core, where it forms SG stars. The SG subsystem emerging from this process is initially strongly concentrated in the cluster innermost regions and its structural properties are largely independent of the FG initial properties. We also present the results of a model in which pristine gas contributes to the SG formation. In this model a very helium-rich SG population and one with a moderate helium enrichment form; the resulting SG bimodal helium distribution resembles that observed for SG stars in NGC 2808.

By means of *N*-body simulations, we then study the two-population cluster dynamical evolution and mass loss. In our simulations, a large fraction of FG stars are lost early in the cluster evolution due to the expansion and stripping of the cluster outer layers resulting from early mass loss associated with FG supernova (SN) ejecta. The SG population, initially concentrated in the innermost cluster regions, is largely unscathed by this early mass loss, and this early evolution leads to values of the number ratio of SG to FG stars consistent with observations. We also demonstrate possible evolutionary routes leading to the loss of most of the FG population, leaving an SG-dominated cluster. As the cluster evolves and the two populations mix, the local ratio of SG to FG stars, initially a decreasing function of radius, tends to a constant value in the inner parts of the cluster. Until mixing is complete, the radial profile of this number ratio is characterized by a flat inner part and a declining portion in the outer cluster regions.

Key words: hydrodynamics – methods: *N*-body simulations – stars: chemically peculiar – globular clusters: general.

1 INTRODUCTION

The common paradigm that globular clusters (GCs) are examples of 'simple stellar populations' (SSP), assemblies of stars born all at the same time and sharing identical chemical composition, had until a few years ago only one noticeable exception: ω Cen, the most massive cluster, whose stars show a large spread in metallicity. Today, the situation is much more complex, and it is now clear that practically none of the GCs so far examined in detail is an SSP. Even when all the stars in a single GC share the same Fe abundance, star-to-star differences in the abundances of lighter elements are found.

⋆E-mail: annibale.dercole@oabo.inaf.it

These differences concern light-element abundances: in a relevant fraction of cluster stars, they look like the result of nuclear processing through proton capture reactions at high temperature (CN, ON, NeNa and MgAl cycles). In particular, O–Na and Mg–Al anticorrelations are found for stars at different stages of their evolution, from the red giant branch to the main sequence (MS) (e.g. Gratton, Sneden & Carretta 2004). Halo field stars with the same metallicity do not show such huge variations (Kraft 1994). This leads us to attribute the anomalous composition to the fact that these stars formed in a dense GC environment, and that nuclear processing in a first stellar generation (hereafter FG), has been followed by a subsequent episode of star formation, creating a second stellar generation (hereafter SG) from matter including this processed gas.

An additional ingredient to the complexity of the new scenario has been added by recognizing that there are at least two clusters, ω Cen and NGC 2808, in which the MS morphology shows that a non-negligible fraction of the stars ($\sim$25 per cent in ω Cen, $\sim$15 per cent in NGC 2808) populate a 'blue MS' which can only be interpreted as a very helium-rich MS (Bedin et al. 2004; Norris 2004; D'Antona et al. 2005; Piotto et al. 2005). The extreme helium population must also be very *homogeneous*, both in helium and metal content, since in both clusters the blue MS is well detached from the rest of the MS. Piotto et al. (2007) have shown that the MS of NGC 2808 is actually made up of three different sequences: a normal MS, a population with somewhat enriched helium ($Y \sim 0.30$) and a very helium-rich one ($Y \sim 0.35$–0.40). In ω Cen the 'normal' MS is actually made up of sequences with different metal content, as also shown by the complexity of the subgiant branch(es) (e.g. Villanova et al. 2007). In addition to ω Cen and NGC 2808, the two massive clusters NGC 6441 and NGC 6388 apparently also harbour a very high helium population, including $\sim$10 and $\sim$20 per cent of stars, respectively. In this case the evidence comes from the high-$T_{\rm eff}$ extension of the horizontal branch (HB; Busso et al. 2007; Caloi & D'Antona 2007; Yoon et al. 2008), a very peculiar occurrence at the high metallicity of these clusters (Rich et al. 1997), and it is not clear whether the very high helium population is as homogeneous as it is in the previous cases.

Observationally, it appears that these extreme Y sequences are present only in the most massive clusters (Piotto et al. 2007). A moderately helium-rich population ($0.26 < Y < 0.30$), on the other hand, is present in most GCs, largely independent of the total cluster mass. The observational spectroscopic evidence resides mainly in the existence of similar Na–O anticorrelation – also among the unevolved stars – in all the clusters so far examined (see e.g. the summary by Carretta et al. 2006) although the most extreme Na–O anomalies are present only in clusters that also show extreme high-$T_{\rm eff}$ extensions of the HB (see Carretta et al. 2007). These results, based generally on spectroscopy of a few stars, have been recently confirmed by the analysis of larger samples of 30–100 stars per cluster (Carretta & Bragaglia 2008). The indications coming from the analysis of the CNO anomalies are similar (for a summary, see e.g. Cohen, Briley & Stetson 2005).

Photometrically, this non-extreme population cannot be easily isolated in the MS photometry, mainly because the moderately helium-rich isochrones merge with the standard isochrones in the turnoff region (D'Antona et al. 2002; Salaris et al. 2006), but also because, in general, these SG stars do not have an unique value of Y (e.g. Lee et al. 2005; Caloi & D'Antona 2007). Nevertheless, these stars show up quite prominently in the HB morphology, which amplifies the mass differences (due to the initial helium content) among stars of the same age (D'Antona et al. 2002; D'Antona & Caloi 2004).[1] It is important to notice that, according to the detailed HB modelling by Caloi & D'Antona (2007) (see also D'Antona & Caloi 2008), also in NGC 6441 and NGC 6388 the total SG population includes $\sim$60 per cent of the total number of stars, and is therefore much larger than just the very high helium fraction population.

The interpretation of the HB morphologies in terms of helium enrichment, coupled with the spectroscopic information indicating that the helium-rich samples probably coincide with the sample of stars showing the Na–O anomalies (e.g. Carretta et al. 2006), lead us to conclude that, in the clusters so far examined, the percentage of stars of the SG is generally $\sim$40–60 per cent (D'Antona & Caloi 2008).

For the clusters having mainly blue HBs, there are even indications that they may contain only- or mainly SG stars (D'Antona & Caloi 2008). In an analysis of the relative magnitude locations of the turnoff, red giant 'bump' and HB, Caloi & D'Antona (2005) have provocatively suggested this possibility for M13, the cluster showing the broadest range of chemical anomalies (Sneden et al. 2004). In addition, some clusters in which the tightness of the evolutionary sequences in the HR diagram (e.g. the relatively small cluster NGC 6397; King et al. 1998; Richer et al. 2006) or the short extent of the HB (e.g. the massive GC M53; D'Antona & Caloi 2008) indicate that they indeed represent SSPs, might be dominated by a homogeneous SG. For example, in NGC 6397 only three out of 14 scarcely evolved stars examined by Carretta et al. (2005) are normal in their nitrogen content. In the others, [N/Fe] $\sim$ 1–1.7, showing CN and ON processing in stars that should not show it. The blue HB of M53 can easily be described as uniparametric (D'Antona & Caloi 2008), but its integrated spectrum shows a strong nitrogen enhancement with respect to field halo stars (Li & Burstein 2003). In conclusion, some 'normal' blue–HB GCs (with typical current masses of a few $\times 10^5$ M$_\odot$) should be considered self-enriched, and any model for the formation and evolution of multiple population clusters must be able to explain the observed large SG population and the cluster-to-cluster variations in the SG/FG number ratio.

Both massive asymptotic giant branch (AGB) stars (Cottrell & Da Costa 1981; Ventura et al. 2001) or 'fast rotating' massive stars (FRMS; Maeder & Meynet 2006; Decressin et al. 2007a) have been proposed as possible progenitors of the SG. The most critical point, common to both scenarios, is the following: for a standard initial mass function (IMF) of the FG, such as a Salpeter or Kroupa IMF, the gas ejected by the massive stars during the phase of H-burning, or the gas contained in the envelopes of massive AGBs (D'Antona & Caloi 2004; Bekki & Norris 2006), is too scarce to form a large SG population. Two solutions to this conundrum have been suggested: either the system had a standard IMF but it was initially much more massive – at least a factor of 10 more massive, under very conservative assumptions (see Section 3.1) – than today's GC (D'Antona & Caloi 2004; Bekki & Norris 2006; Prantzos & Charbonnel 2006; D'Antona, Ventura & Caloi 2007; Decressin, Charbonnel & Meynet 2007b), or the system evolves at constant mass and the IMF is highly anomalous (D'Antona & Caloi 2004; Decressin et al. 2007b, see also Downing & Sills 2007 for a dynamical study) and contains a significant number of FG polluters. As we will discuss in Section 4.3, a large initial mass is necessary also in this second scenario if a cluster must have today an approximately equal number of long-lived SG and FG stars (where

[1] The age difference between FG and SG is in any case so small with respect to the total GC age that it is irrelevant for the turnoff evolution.

we define long-lived stars as those having initial masses in the range 0.1–0.8 $M_\odot$).

We reconsider here the problem of GC formation to explain not only the most peculiar very helium-rich population (15–20 per cent in three GCs, 25 per cent in ω Cen), but also the whole SG population (about 40–60 per cent of the current GC stellar content, and possibly even more in the 'blue HB' clusters).

In this work, we follow the idea that the intermediate-mass stars of the FG, starting at 8 $M_\odot$ and extending at most down to ∼4–5 $M_\odot$, lose by stellar winds and the ejection of planetary nebulae matter processed by the hot CNO cycle via hot bottom burning (Na- and Al-rich, O- and Mg-poor) during their AGB evolution, and that an SG forms either from the pure AGB ejecta or from ejecta mixed with pristine gas. While previous work examined the reliability of this model from a chemical point of view, here we focus mainly on its hydrodynamical and dynamical consistency.

In Section 2 we first briefly summarize the state of the art of chemical modelling of the SG, we discuss the reasons why we focus our attention on the scenario in which the AGB stars are the polluters and emphasize the possible role of super-AGB stars.

In Sections 3 and 4, we address this problem by means of one-dimensional (1D) hydro simulations. We show that in the massive AGB epoch, the slow winds collect in a cooling flow driving AGB ejecta to the centre of the cluster, where they form SG stars. Simulations exploring the dependence of our results on the cluster mass, IMF, initial concentration as well as the role of Type Ia supernovae (SNe Ia) and other extra energy sources are also presented in this section.

In Section 5, we explore a model in which the pristine matter is partially re-accreted after the Type II supernova (SN II) explosion stage. The stellar population forming after the accretion shows a lower helium abundance relative to the stars formed earlier from the pure ejecta of the super-AGBs. This may explain the presence of the very high-helium population observed in a few, very massive GCs.

In Section 6, we present the results of a number of *N*-body simulations exploring the subsequent cluster dynamical evolution. We show that the early cluster expansion driven by mass loss due to supernova (SN) ejecta leads to a strong preferential loss of FG stars. Our simulations show that dynamical evolution can lead to values of the ratio of the number of SG to FG stars consistent with those suggested by observational studies. We also show possible evolutionary routes leading to the loss of most of the FG stars, leaving an SG-dominated cluster.

2 THE PROGENITORS OF THE SECOND GENERATION: PREAMBLE

2.1 Why AGB and super-AGB stars

Although the study of the formation and dynamical evolution of multiple population clusters is the main goal of this paper, one of the key assumptions of our investigation is that the SG progenitors are AGB stars, a scenario which has been criticized in a few recent studies aimed at producing a plausible chemical evolution history of GCs. In this section we briefly review a number of recent studies of the chemical modelling of SG stars and discuss why the AGB stars (along with the implications of the role of super-AGBs) are still to be considered a key ingredient in any theory for the formation of a SG population.

In the last decade, attention has been focused mainly on the AGB scenario, based on the simple idea that the AGB winds are slow enough to be retained in the potential well of the cluster, and that these winds are processed through the hot CNO cycle by 'hot bottom burning' (Cameron & Fowler 1971; Sackmann & Boothroyd 1992) at the bottom of the convective envelope (Ventura et al. 2001). Many different groups have addressed the computation of suitable models for the chemical anomalies, and a number of results apparently do not support this scenario (Fenner et al. 2004; Karakas et al. 2006; Choi & Yi 2008), while the model presented in Bekki et al. (2007) is in only partial agreement with the data.

The model of SG formation by the contribution of FRMS has been proposed much more recently (Maeder & Meynet 2006; Prantzos & Charbonnel 2006; Decressin et al. 2007a,b) and, while it is not our goal to dismiss the FRMS scenario, we emphasize that many of its aspects are still to be fully explored. In particular, the main assumptions of this model are particularly stringent: all the stars must rotate at break-up speed, both to achieve a deep rotational mixing of CNO processed matter in the envelope and to inject, with small or zero ejection velocity, the CNO processed ejecta into the cluster, where they mix with the intracluster pristine matter (Decressin et al. 2007a). Conversely, the high-velocity winds during the helium-core burning phase and the SN ejecta must leave the cluster without any interaction with the remnant gas. The hydrodynamical and dynamical aspects of the FRMS scenario have not been studied, and a recent Very Large Telescope (VLT) Fibre Large Array Multi Element Spectrograph (FLAMES) survey of massive stars, studying the nitrogen abundance and the rotational velocity of 135 B-type stars in the Large Magellanic Cloud (LMC; Hunter et al. 2008), has found a number of unenriched fast rotators and cast some doubt on the efficiency of rotational mixing.

As far as the AGB scenario is concerned, it is important to emphasize the following points. In discussing AGBs, we generally think of the low-mass, thermally pulsing AGBs that go through long series of thermal pulses and dredge-up episodes, so that they are generally rich in carbon and s-process elements. But these are not the AGB stars that can be progenitors of the SG in clusters. Some studies show that the sum of CNO elements is approximately constant among FG and SG stars (Cohen, Briley & Stetson 2002; Cohen & Meléndez 2005). This is possible only if we are dealing with the most massive AGBs, in which the episodes of third dredge-up are small in number, and the temperature at the base of the convective envelope is so large ($>8 \times 10^7$ K) that the ON cycle is active, reducing the O abundance as observed in the anomalous stars. Carretta et al. (2005) find that the CNO abundance is actually somewhat – although not much – larger in the SG stars. The latter data indicate that the third dredge-up (e.g. Iben & Renzini 1983) plays a (small) role, but the dredge-up episodes must be limited in number. Moreover, a few dredge-up episodes do not alter the s-process abundances, so that the lack of s-process enrichment in the SG is not an argument against the AGB polluters.[2]

[2] A different, borderline, situation seems to be present in NGC 1851, whose HR diagram shows a splitting of the subgiant branch (Milone et al. 2008), that can be interpreted as due to two different stellar populations differing in total CNO abundance (Cassisi et al. 2008). This is the only cluster in which a bimodal spread in the abundance of s-process elements has also been found, anticorrelated with the oxygen abundance (Yong & Grundahl 2008). More than others, this case might indicate that the AGB scenario is to be preferred to the FRMS scenario: with respect to most GCs, the SG of NGC 1851 may have been born from somewhat less massive AGBs, for which the effect of the third dredge-up is more clearly evident, both in the total CNO abundance and s-process elements increase.

A confusing issue when discussing the AGB evolution of low-metallicity stars is that the chemical yields based on AGB modelling by different groups differ enormously. The yields based on sets of models computed by Lattanzio's group, widely used for follow–ups and recently published by Karakas & Lattanzio (2007), provide the correct abundance signatures of the SG only for the most massive AGBs ($\sim 7\,M_\odot$), while the yields of Ventura's group, and especially the most recent models by Ventura & D'Antona (2008a,b), look compatible with the anomalies down to $\sim 5\,M_\odot$. The mass-loss rate formulation, the nuclear reaction rates and other details such as the treatment of core overshooting in the phases previous to the AGB are all relevant to the determination of yields (e.g. Ventura & D'Antona 2005b). However, the most important difference among the physical inputs to these two sets is the treatment of superadiabatic convection, which affects the temperature stratification of models in the phase of 'hot bottom burning' and the stellar luminosity and mass loss (Ventura & D'Antona 2005a). A 'more efficient' convection model – like the Full Spectrum of Turbulence (FST) model (Canuto, Goldman & Mazzitelli 1996) adopted in Ventura's computations – destroys oxygen more efficiently, shortens the AGB lifetime and reduces the number of thermal pulses and the effect of the third dredge-up for a wider range of initial masses than in Karakas & Lattanzio (2007). Thus, the AGB yields are very model dependent, and the models of chemical evolution based on these yields are very model dependent too, so that negative results can not necessarily be taken as falsification of the AGB progenitor scenario.

The first complete model for the chemical anomalies by Fenner et al. (2004) shows that self-enrichment by AGBs is at variance with most of the observational anomalies, but this result could be easily predicted, as it is based on the Karakas & Lattanzio (2007) set.

More recently, attention has been mostly devoted to explaining the presence of a population with extreme helium content, although, as we have noted, this population is only the tip of the iceberg of the SG, and it is present only in the most massive clusters. As ω Cen shows the signatures of a complex chemical history (see e.g. Romano et al. 2007, for a summary of the extensive observational studies of ω Cen), and its formation took place most likely over an extended period (2–4 Gyr; e.g. Stanford et al. 2006), several attempts have been made to understand its very high helium population by means of standard chemical evolution models. Romano et al. (2007) showed that the evolution of ω Cen cannot be understood in terms of a 'closed box' model, and that, also after relaxing this hypothesis, the helium-to-metal enrichment $\Delta Y/\Delta Z \sim 70$ of the blue MS stars of this system cannot be attained, even with the very high helium yields of the winds of massive stars. Models of ω Cen taking into account inhomogeneous pollution by SNe Ia can reduce (by $\sim$40 per cent) but not eliminate the extra amount of helium needed to explain the presence of the blue MS (Marcolini et al. 2007).

Karakas et al. (2006) assumed that the helium yields come from the massive AGBs, and that the IMF is indeed peaked at these masses, in order to maximize the effect of the self-enrichment. In this case, they indeed could find a fraction of SG stars with Y up to $\sim$0.35, but this is accompanied by a very large CNO enrichment, that is not observationally found. This result again depends on the models adopted to describe the helium yield: only the Karakas & Lattanzio (2007) models provided helium abundances as large as $Y \gtrsim 0.35$ in the AGB ejecta, and this value was partially achieved at the 'second dredge-up' (Iben & Renzini 1983), and partially by the third dredge-up during the thermal pulse phase. The third dredge-up of course also alters the total CNO abundance in the envelopes.

Only recently has it become clear that a very high helium content ($Y \sim 0.38$) can be achieved already after the second dredge-up in the envelopes of the most massive 'super-AGB' stars (Siess 2007a). The sum of the CNO abundances can remain close to the initial value during the following AGB thermal pulse phase, as the efficiency of third dredge-up is limited, because the helium luminosity during the thermal pulses is weak (Siess 2007b). Unfortunately, full models through the super-AGB thermal pulse phase are not yet available, but it is clear that, in principle, it is possible to achieve high helium abundances without enhancing the CNO. Following this idea, Pumo, D'Antona & Ventura (2008) suggest that the extreme helium-rich stars are formed directly from the ejecta of super-AGB stars.

Finally, Choi & Yi (2008), even adopting a model that maximizes the possible role of AGBs, tried and failed again to model the ω Cen $\Delta Y/\Delta Z \sim 70$ for 30 per cent of its population, concluding that 'alternative processes are desperately called for.' Again they do not include the most recent yields for super-AGBs in their computations, and use an almost closed box model, assuming that for the formation of the FG a fraction from 0.5 to 1 of the available gas is used. Thus the gas from which the SG is formed comes at most from half of the mass of the pristine gas plus the FG ejecta, or entirely from the FG ejecta. Under this hypothesis, for any reasonable shape of the IMF, the helium-rich AGB ejecta cannot reach 30 per cent of the total cluster mass, as we will discuss again in Section 3.1. In fact, modelling must be able to predict at least a factor of 10 mass loss from the FG, to produce the desired number ratio of SG/FG stars of $\sim$1.

2.2 The super-AGB phase

In the exploratory models presented in this work, we do not consider in detail the peculiarity of the super-AGB evolution, although we plan to include it in much more detail in subsequent work dealing explicitly with the chemistry of the ejecta. However, we discuss briefly here the super-AGB phase and its possible evolutionary outcomes, as it has consequences for our interpretation of these preliminary model results too. The minimum mass evolving into a core-collapse SN is today referred to as $M_{\rm mas}$, to distinguish it from the limit $M_{\rm up}$, representing the minimum mass for carbon ignition, below which stars evolve into C–O white dwarfs (WDs). Stars in the mass range $M_{\rm up} < M < M_{\rm mas}$ are called super-AGBs, and ignite carbon off-centre in semidegenerate conditions, but are not able to ignite hydrostatic neon burning in the resulting O–Ne core. Consequently, degeneracy increases in the core, and these stars may undergo thermal pulses (e.g. Iben, Ritossa & Garcia-Berro 1997; Ritossa, García-Berro & Iben 1999; Siess 2006) and lose mass as 'normal' (but quite massive and luminous) AGBs, the difference being the core composition (O–Ne versus C–O) and core mass ($\geq 1.05\,M_\odot$).

As mentioned in Section 2.1, super-AGBs may play an important role in the evolution of proto-GCs. Siess (2007a) shows that their helium content in the envelope may reach the values $Y = 0.36$–0.38, reasonably consistent with the highest helium content found in the extreme populations of a few GCs, and Pumo et al. (2008) suggest that they are in fact the progenitors of the extreme He populations.

The fate of super-AGBs depends on the competition between mass loss and core growth (Poelarends et al. 2008; Siess 2007a): if mass loss wins, they evolve into massive O–Ne WDs (Nomoto 1984); if the core reaches the Chandrasekhar mass, they evolve into electron capture supernovae (ecSNe), electrons being captured on the Ne nuclei. Thus also stars below $M_{\rm mas}$ may explode as SNe, but these events are at least a factor of 10 less energetic than SNe II ($\leq 10^{50}$ erg;Dessart et al. 2006) and also a factor of 10 smaller than

SNe Ia. In fact, it has been recently proposed that practically all the neutron stars (NSs) today present in GCs are born from ecSNe: due to their lower energy output, it is also probable that the newborn NS receives a proportionally smaller natal kick, allowing it to remain bound to the cluster (Ivanova et al. 2008).

The presence of super-AGBs has an interesting consequence on the cluster evolution: the fate of super-AGBs in fact is either to end their life quietly as O–Ne WDs, or to explode as ecSN (either directly, or due to accretion-induced collapse induced by mass transfer by a binary companion). In both cases, until O–Ne cores are formed, we do not have SN Ia explosions, that are due to the explosion of C–O WDs reaching the Chandrasekhar mass by accretion. These events can take place only after C–O WDs are formed in the cluster, when masses $M < M_{\rm up}$ evolve. Consequently, the epoch during which the super-AGBs evolve is probably the quietest period of the cluster's life, perturbed at most by ecSNe explosions, either in single stars or by accretion-induced collapse, and in any case not so energetic to alter either the gas evolution, as we will see in the hydrodynamical simulations, or its chemistry, as the whole core remains locked into the remnant NS. We refer the reader to Siess (2007a) for a careful study of $M_{\rm mas}$ as a function of the stellar metallicity. His value for the typical metallicity of GCs showing multiple stellar populations is $\sim 10\,{\rm M}_\odot$ for models not including core overshooting. For models with moderate core overshooting this value is reduced by $\sim 1\,{\rm M}_\odot$, thus to $9\,{\rm M}_\odot$. The value of $M_{\rm up}$ from the models by Ventura & D'Antona (2008a,b) is $\sim 6.3\,{\rm M}_\odot$ evolving at $\sim$65 Myr (see table 1 in Ventura & D'Antona 2008a). These latter models provide yields consistent with the GC chemical anomalies down to the evolution of $5\,{\rm M}_\odot$, evolving at an age of $\sim 10^8$ yr. In this scheme, in summary, the SG may be formed by super-AGBs down to $M > 6.3\,{\rm M}_\odot$, and by AGBs down to $\gtrsim 5\,{\rm M}_\odot$. In Section 4.4, we choose 40 Myr as the minimum age to start SN Ia explosions, in order to maximize their possible role. This limit shifts to $\gtrsim$65 Myr for the Ventura & D'Antona (2008a) models, allowing a longer time for the formation of the SG.

2.3 Post-AGB evolution

We now consider whether the post-AGB evolution can play a role in the formation of the SG. In fact, after the loss of the envelope, the remnant hot cores evolve toward the WD stage, reaching very high values of $T_{\rm eff}$ and thus becoming powerful sources of ultraviolet (UV) photons, acting as extra energy sources and potentially affecting the behaviour of the AGB gas. A study of the possible dynamical role played by extra energy sources is presented in Section 4.5.

Post-AGB evolution of the massive AGB core begins when the envelope mass is reduced below a critical value that does not allow stationary H burning on the AGB, so that the residual envelope contracts (at the constant luminosity dictated by the core mass itself) and the star becomes increasingly hotter. Planetary nebula excitation occurs at $T_{\rm eff} > 30\,000$ K, when UV photons begins to be emitted. The critical envelope mass is a strong function of the core mass. In addition, the stellar luminosity is also increasing with the core mass. Based on the computations by Paczyński (1971), Iben (1985) showed that the 'fading time' that is required for the luminosity to fall by a factor of 10 after the star has reached $T_{\rm eff} = 30\,000$ K is proportional to $M_{\rm core}^{-10}$, so that, while it is $>10\,000$ yr at the core masses of typical planetary nebula nuclei ($0.6\,{\rm M}_\odot$), it is only a few hundred years for the core masses 1.0–1.3 $\rm M_\odot$ that are remnants of the possible progenitors of the SG we are considering (see also Van Winckel 2003, for a review). These objects, being so short-lived, are not a significant extra energy source capable of affecting the gas dynamics during the evolutionary phase we are considering.

3 INPUTS TO THE GAS DYNAMICAL MODELS

3.1 The framework

The model building is as follows. The present GC is assumed to be composed of two stellar components, namely the FG and the SG stars. Its mass can thus be written as $M_{\rm now} = M_{\rm FG,now} + M_{\rm SG,now}$, where $M_{\rm FG,now}$ and $M_{\rm SG,now}$ represent the amount of mass today in long-lived FG and SG stars, respectively (recall, as mentioned in Section 1, that we define long-lived stars as those having initial masses in the range $0.1 < M/{\rm M}_\odot < 0.8$). The value of x (in the range $0 \le x \le 1$) indicates the relative abundance of the two populations: $M_{\rm FG,now} = xM_{\rm now}$ and $M_{\rm SG,now} = (1-x)M_{\rm now}$.

The FG is assumed to be already in place with an initial mass $M_{\rm FG}$ following a continuous King radial profile

$$\rho_* = \rho_0 \left[1 + \left(\frac{r}{r_{\rm c}}\right)^2\right]^{-1.5} \quad (1)$$

up to the truncation radius $r_{\rm t}$. These stars have masses in the range $0.1 < M < 100\,{\rm M}_\odot$ distributed according to a Kroupa IMF $\Phi(m)$ (Kroupa, Tout & Gilmore 1993). The mass fraction δ of long-lived FG stars is given by

$$\delta = \int_{0.1}^{0.8} m\Phi(m)\,{\rm d}m. \quad (2)$$

For our assumed IMF, we find $\delta = 0.5$.

The evolutionary times are taken from Padovani & Matteucci (1993). We will consider as progenitors of the SG the stars of masses below the limit for core-collapse SN (SN II) explosion, here assumed to be $M = 8\,{\rm M}_\odot$. We discussed in Section 2.2 that, for the metallicities of GCs, this limit should probably be shifted to $\sim 9\,{\rm M}_\odot$ for models including core overshooting, but the precise choice does not make an important difference to the global picture.

We start our calculations at $t = 28$ Myr, when all the SNe II have exploded, clearing the GC of all the pristine gas (we will reconsider the possible role of pristine gas in Section 5). At this stage, $M_{\rm FG}$ is reduced by an amount $\Delta M_{\rm FG} = \epsilon M_{\rm FG}$; for a Kroupa IMF $\epsilon = 0.08$, but it can be much larger for flatter IMFs (see Section 4.3). The SG stars form from the ejecta of the AGB stars of the FG during a period of time $\Delta t_{\rm f}$, which must be long enough to allow the formation of a substantial SG population, but not so long as to include evolution of stars of masses $M \le 4$–$5\,{\rm M}_\odot$, which do not provide yields compatible with the observed chemical anomalies. The value adopted in our simulations, $\Delta t_{\rm f} = 100$ Myr, satisfy this constraint and only stars with initial masses $M > 4\,{\rm M}_\odot$ contribute to the SG formation.

The amount of gas returned by the FG in this period is $\Delta M_{\rm g} = \beta M_{\rm FG}$, where, for Kroupa IMF, $\beta = 0.05$. Following Prantzos & Charbonnel (2006) and Decressin et al. (2007a), we assume that SG stars have masses within the range 0.1–0.8 $\rm M_\odot$, and thus are all still present today. In the working hypothesis that all the gas forms stars, i.e. that the star formation efficiency is $\eta = 1$, the SG mass is therefore $M_{\rm SG,now} = \Delta M_{\rm g} = \beta M_{\rm FG}$.

We stress that our assumption of a SG IMF skewed toward low masses is made to minimize the FG mass: if stars with $M > 0.8\,{\rm M}_\odot$ are assumed to also be formed, the required ejecta mass, and thus $M_{\rm FG}$, would be larger. The assumption of a flatter IMF, with its larger mass return, does not lead to a significant lowering of $M_{\rm FG}$. In fact,

in this case, the number of long-lived FG stars would decrease, and thus a large value of $M_{\rm FG}$ is still needed to obtain a significant quantity of them (see Section 4.3). It is worth noticing that while SG stars more massive than $0.8\,{\rm M}_\odot$ can be included in our model, stars with masses larger than $8\,{\rm M}_\odot$ must be excluded; these stars explode as SNe II and would sweep out the gas returned by the FG stars, preventing the formation of a substantial stellar SG. In any case, we point out that formation of (only) low-mass stars has been invoked also in the cooling flow occurring in elliptical galaxies (e.g. Mathews & Brighenti 1999) which are a scaled version of the cooling flows taking place in our GC models (see Section 4.1).

From all the above, it follows that $M_{\rm FG} = fM_{\rm now}$, where $f = (1 - x)/\beta$. For a Kroupa IMF, and assuming $x = 0.5$ as a rule of thumb, we obtain $M_{\rm FG} = 10M_{\rm now}$. Thus, a GC with a current mass $M_{\rm now}$ originates from a FG 10 times larger, or even larger if the gas is not completely turned into stars (or if the IMF of the SG is not limited to $0.8\,{\rm M}_\odot$). This huge extra amount of mass must be lost in the successive evolution of the cluster. We postpone the discussion of this point to Section 6, and describe in the next sections the dynamics of the gas returned by the FG and the formation of the SG stars.

3.2 Physical inputs

In order to follow the gas evolution in the GC, we adopt the 1D version of the hydrocode described in Bedogni & D'Ercole (1986) and solve numerically the following equations:

$$\frac{\partial \rho}{\partial t} + \nabla \cdot (\rho \boldsymbol{v}) = \alpha\rho_* - \nu\frac{\rho}{t_{\rm sf}}, \tag{3}$$

$$\frac{\partial \boldsymbol{m}}{\partial t} + \nabla \cdot (\boldsymbol{m} \otimes \boldsymbol{v}) = -(\gamma - 1)\nabla E - \boldsymbol{g}\rho - \nu\frac{\boldsymbol{m}}{t_{\rm sf}}, \tag{4}$$

$$\frac{\partial E}{\partial t} + \nabla \cdot (E\boldsymbol{v}) = -(\gamma - 1)E\nabla \cdot \boldsymbol{v} - \nu\frac{E}{t_{\rm sf}} - L + S. \tag{5}$$

In the above equations, $\boldsymbol{v}$, ρ, $\boldsymbol{m}$ and E represent, respectively, the gas velocity and the densities of the gas mass, momentum and internal energy. The gravitational acceleration $\boldsymbol{g}$ is due to both FG and SG stars, as well as to the gas. The ratio of the specific heats is $\gamma = 5/3$. Given the assumptions described above, the mass loss occurs only from FG stars at the specific rate $\alpha = \dot{M}_{\rm FG}/M_{\rm FG}$, and ρ_* thus represents the FG stellar density. The mass-loss rate $\dot{M}_{\rm FG}$ is computed following Ciotti et al. (1991), adapted to the IMF chosen for the present case. The star formation rate (SFR) is characterized by the time-scale $t_{\rm sf} = \max(t_{\rm cool}, t_{\rm ff})$, where $t_{\rm cool}$ and $t_{\rm ff}$ are the cooling time and the free-fall time of the gas, respectively; it is usually $t_{\rm cool} \ll t_{\rm ff}$ and thus $t_{\rm sf} \propto t_{\rm ff} \propto \rho^{-0.5}$. The arbitrary parameter ν summarizes our uncertainties about star formation, but we find that our results are essentially independent of its value (the reason for this is discussed in Appendix A); as a consequence, all the models presented in this paper have $\nu = 1$. We stress, however, that the star formation is allowed only in regions where the gas is converging. For this reason we set

$$\nu = \begin{cases} 0, & \nabla \cdot \boldsymbol{v} \geq 0, \\ 1, & \nabla \cdot \boldsymbol{v} < 0. \end{cases} \tag{6}$$

Radiative losses are given by $L = n^2\Lambda(T)$, where n and T are the number density and the temperature of the gas, respectively, and $\Lambda(T)$ is the cooling curve as given by Rosen & Bregman (1995). The source term S takes into account the heating of the gas due to the feedback of the stars:

$$S = 0.5\alpha\rho_* \left(3\sigma^2 + v^2 + v_{\rm w}^2 + 2q\right). \tag{7}$$

The first three terms in the above equation are due to the thermalization of the kinetic energy of the AGB winds, where v is the gas velocity, σ is the 1D velocity dispersion of the FG stars and $v_{\rm w} = 2 \times 10^6\,{\rm cm\,s^{-1}}$ is the wind velocity of the AGB stars (e.g. Marshall et al. 2004). We also computed a set of models in which an ad hoc heating source q of stellar origin is added (see Section 4.5).

Assuming that the SNe Ia belonging to the FG start to explode with a delay of 80–100 Myr, we are allowed to neglect their effect in our simulations, and equation (7) represents the total energy source of the system. If, however, such a delay is shorter, the repercussions of the stellar explosions must be taken into account (see Section 4.4).

We conclude this section by pointing out that in our hydrodynamical simulations we have assumed a static stellar potential. As discussed in Section 6, the cluster is expected to expand during its early evolution in response to the early mass loss due to SN ejecta. In a further study now underway, we will explore the role of the early expansion of the cluster driven by primordial gas loss and SN II ejecta on the formation and final structural properties of the SG system. We have carried out a number of preliminary simulations with initial conditions as in the standard case, for a FG system expanding homologously and in isolation; the results seem to indicate that the central gas and SG stellar densities and, in general, the conclusions concerning the SG properties for the standard case are not significantly affected by the cluster expansion.

3.3 The energy budget

The energy required per unit time to extract from the GC the gas returned at rate α by the FG is (see Ciotti et al. 1991)

$$L_{\rm g} = -\alpha(t)\int_0^{r_{\rm t}} 4\pi r^2 \rho_{\rm FG}(r)\phi_{\rm FG}(r)\,{\rm d}r, \tag{8}$$

where $\rho_{\rm FG}(r)$ and $\phi_{\rm FG}(r)$ are the radial profiles of the FG stellar density and gravitational potential, respectively. The energy input linked to such mass return and due only to the stellar velocity dispersion is

$$L_\sigma = \frac{3}{2}\alpha(t)\int_0^{r_{\rm t}} 4\pi r^2 \rho_{\rm FG}(r)\sigma^2(r)\,{\rm d}r. \tag{9}$$

By definition, these two equations can be written as

$$L_{\rm g} = 2\alpha(t)|U|, \tag{10}$$

$$L_\sigma = \alpha(t)K, \tag{11}$$

where U and K are the binding energy of the GC and the kinetic energy of the stars, respectively. If the FG is in virial equilibrium, then $L_{\rm g} = 4L_\sigma$. This is a general result independent of the amount of mass and of the shape of the FG potential well. The first three terms in equation (7) are of the same order of magnitude; therefore, in principle an extra source $Q \geq L_\sigma$ would be enough to revert the cooling flow into a wind, thus halting the SF. However, because of the large radiative losses occurring in a cooling flow, a wind can start only for sources much larger than L_σ (see Section 4.5). It must also be pointed out that, for sufficiently small $M_{\rm FG}$, the energy of the AGB winds may vent from the GC at least part of the gas returned by the stellar FG (see Section 4.2).

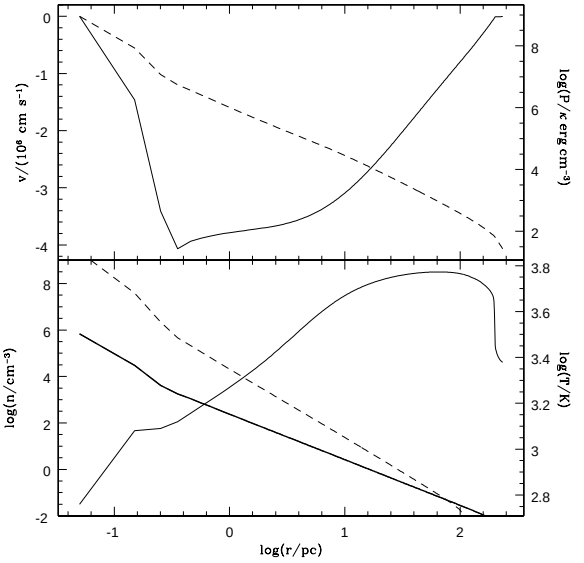

Figure 1. Radial profile of several quantities at $t = 100$ Myr for the standard model. Upper panel: gas velocity (solid line) in units of 10^6 cm s^{-1} and pressure (dashed line) in units of κ erg cm^{-3}, where κ is the Boltzmann's constant. Lower panel: gas density (thick solid line), gas temperature (thin solid line), SG stellar profile produced by the simulation (dashed line).

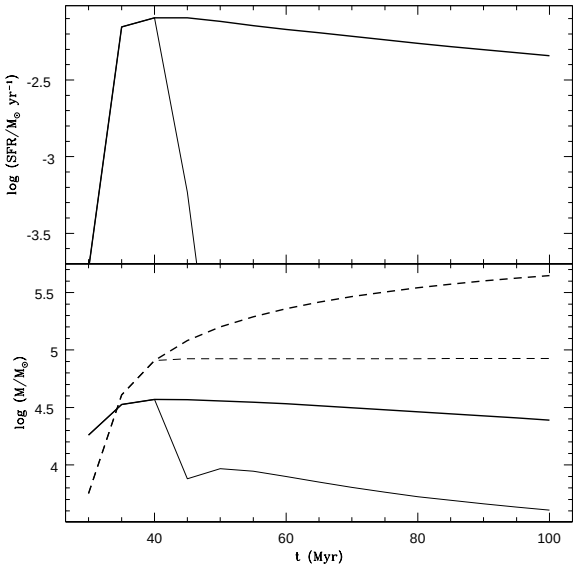

Figure 2. Evolution of the standard model. Upper panel: SFR evolution. Lower panel: temporal profile of the amount of gas (solid line) and SG stars (dashed line). The thick lines refer to an evolution in absence of SNe Ia. In both panels the thin lines indicate the effect of SN explosions starting at $t =$ 40 Myr and occurring every 5×10^4 yr.

4 RESULTS

4.1 The standard model

For our standard model we assume a FG stellar mass $M_{\rm FG} = 10^7\,{\rm M}_\odot$ in order to describe a GC with a current mass $M_{\rm now} = 10^6\,{\rm M}_\odot$, as discussed in Section 3.1. This initial stellar population follows a King radial profile with the parameters below (see equation 1): $\rho_0 = 10^3\,{\rm M}_\odot\,{\rm pc}^{-3}$, $r_{\rm c} = 6.3$ pc and $r_{\rm t} = 200$ pc. The truncation radius of the model coincides with its tidal radius at a distance of 4 kpc from the Galactic Centre.

Fig. 1 shows the radial profile of several quantities at $t = 100$ Myr, when the mass of the SG stars has grown to $M_{\rm SG} = 4.45 \times 10^5\,{\rm M}_\odot$. The upper panel shows that the fluid velocity is negative over the entire cluster; radiative losses prevail over the heating source, particularly in the central region where the amount of gas shed by the FG is larger and causes significant radiative cooling, which strongly increases with the gas density (see Section 3.2). Consequently, the gas pressure falls and gravity succeeds in driving the gas inward, establishing a cooling flow from the start. This gas accumulates in the centre, as shown by the thick solid line in the lower panel of Fig. 1. The SG stars forming from this gas are thus more concentrated than the FG stars; their distribution is indicated by the dashed line, terminating at radius $r \sim 100$ pc, half of the assumed $r_{\rm t}$. The lower panel also shows the temperature profile increasing with radius, as expected in a cooling flow.

Since $t_{\rm sf} \propto \rho^{-0.5}$ (see Section 3.2), the SFR is proportional to $\rho^{1.5}$ (see equation 3), and the SG stars form preferentially in the central region, where they are highly concentrated. The dashed line in the lower panel of Fig. 1 indicates the radial distribution of the SG stars as they form from the gas.

The thick lines in Fig. 2 show the gas and the SG mass evolution, as well as the time evolution of the SFR. Although the star formation process is rather effective, we point out that $M_{\rm SG} = 5 \times 10^5\,{\rm M}_\odot$ (corresponding to the case $x = 0.5$) is attained only at $t = 120$ Myr. Actually, the final value of the SG mass depends on the time at which a suitable number of SNe Ia belonging to the FG start to explode, removing gas from the cluster and inhibiting further star formation. We will discuss the role of SN Ia explosions further in Section 4.4.

4.2 Model with a lower initial FG mass

We have run a model similar to the standard one, but with a stellar FG mass $M_{\rm FG} = 10^6\,{\rm M}_\odot$. In this case, the initial parameters are $\rho_0 = 1.08 \times 10^3\,{\rm M}_\odot\,{\rm pc}^{-3}$, $r_{\rm c} = 2.85$ pc and $r_{\rm t} = 90$ pc (also in this case the truncation radius corresponds to the tidal radius at a distance of 4 kpc from the Galactic Centre). In principle, since the gravitational potential, mass return rate and L_σ all depend linearly on $M_{\rm FG}$, the gas behaviour in this case should simply be a scaled version of the cooling flow developed in the standard case, with lower velocities, temperatures and densities. However, the source term S (see equation 7) depends also on $v_{\rm w}$, the velocity of the AGB winds, which does not scale with $M_{\rm FG}$. Moreover, radiative losses depend quadratically on the gas density (see Section 3.2). For these reasons, the self-similar scaling of the models with $M_{\rm FG}$ breaks when $M_{\rm FG}$ is low enough to generate a stellar velocity dispersion σ a factor of a few lower than $v_{\rm w}$ and a mass return from the FG stars such that the gas density is not so large to provide effective radiative cooling. In the present model the source term prevails on the radiative losses only at the outskirts of the cluster; as a consequence, a partial wind forms, with the stagnation point located at $r = 23$ pc (see Fig. 3). For this reason the SG stellar population is relatively more concentrated than in the standard case, extending only out to $r = 0.18 r_{\rm t}$. However, the comparison between Figs 2 and 4 (thick lines) shows that the global behaviour of gas and SG stars are similar in the two models.

4.3 Model with a flatter IMF

Following D'Antona & Caloi (2004), one can assume a flatter IMF for the FG in order to get a larger number of giant stars at early

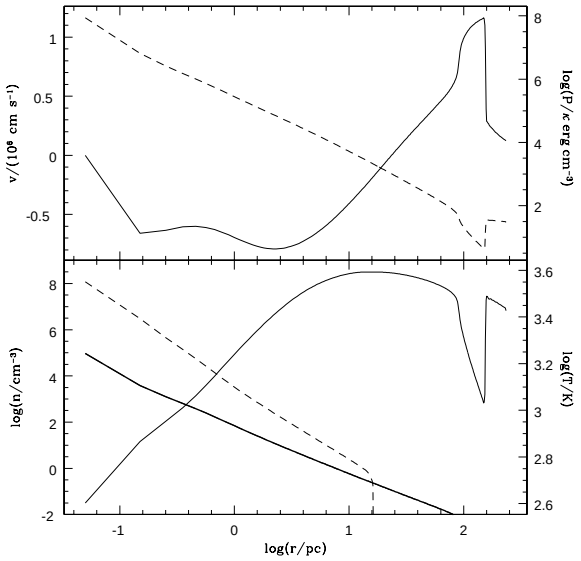

Figure 3. As Fig. 1, but for $M_{\rm FG} = 10^6\,{\rm M}_\odot$.

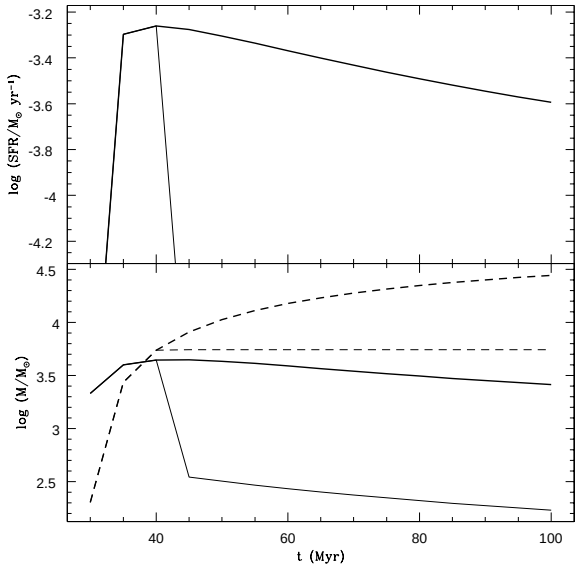

Figure 4. As Fig. 2, but for $M_{\rm FG} = 10^6\,{\rm M}_\odot$.

epochs. In this way, the larger amount of gas returned by such stars would facilitate the formation of the SG. To explore this scenario, we assume that for $M < 5\,{\rm M}_\odot$ the IMF follows a power law with an exponent $s = -1$, while more massive stars follow a Salpeter distribution with $s = -2.35$. The flatter IMF leads to a larger amount of $M_{\rm g}$ and $M_{\rm SG}$ at any time compared to the standard model, as illustrated in Fig. 5 (thick lines).

Repeating for this model the simple analytical calculation of Section 3.1, we obtain $\beta = 0.2, \delta = 0.05$ and $\epsilon = 0.5$. Assuming $x = 0.5$, i.e. that half of the MS stars with $0.1 < M/{\rm M}_\odot < 0.8$ currently in the GC belong to the FG, we have $0.05M_{\rm FG} = 0.5M_{\rm now}$ and thus $M_{\rm FG} = 10M_{\rm now}$. As $\Delta M_{\rm g} = 0.2M_{\rm FG} = 2M_{\rm now}$, the star formation efficiency must be $\eta = 0.25$. In conclusion, also in this case, if one requires the current mass of long-lived SG and FG stars to be similar, the total FG initial mass must be 10 times larger than the current total mass of long-lived stars. However, in this case the cluster must evolve without losing mass because the initial

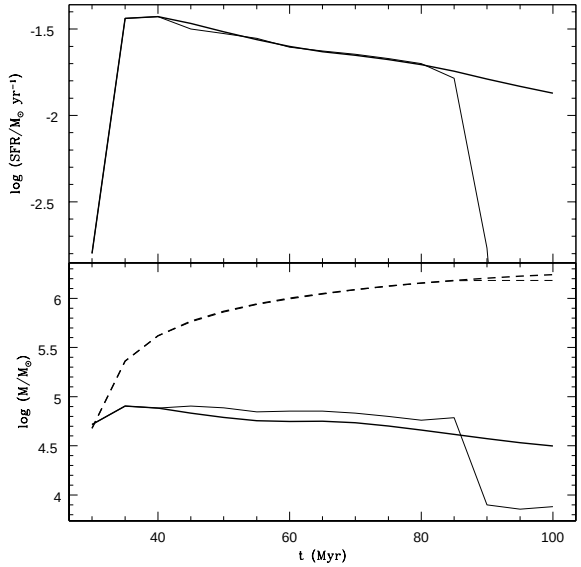

Figure 5. As Fig. 2, but for a flatter IMF (see text).

number of long-lived FG stars is much smaller. We also point out an important difference concerning the relative abundance of stellar remnants (WDs, NSs and black holes) and long-lived MS stars ($0.1 < M/{\rm M}_\odot < 0.8$). Specifically, in both cases at $t \sim 13.5$ Gyr, $M_{\rm rem} \sim 0.15M_{\rm FG}$, but for systems with a flatter IMF the total mass of long-lived stars is smaller and the ratio of the total mass in stellar remnants to the total mass in long-lived stars is much larger (by a factor of $\sim 10^2$) for systems with a flatter IMF.

4.4 Models with SN explosions

In order to understand the effect of SNe Ia in our standard model, we simulated the expansion of SN remnants (SNRs) through the GC. Given the spherical symmetry of the model, we assume that the explosions occur in the centre; such an assumption is reasonable, as in the central region there is a larger density of SN Ia progenitors belonging to the FG. We also assume that the first explosion takes place at the time $t_{\rm pk}$ at which the SN Ia rate quickly reaches its maximum. This time is not unambiguously determined, and its value for a SF of short duration is estimated in the range $40 < t_{\rm pk} < 300$ Myr (Matteucci & Recchi 2001; Mannucci, Della Valle & Panagia 2006). In order to emphasize the effects of the SNe Ia, in the present models we adopt $t_{\rm pk} = 40$ Myr, following the SN Ia rate illustrated by Marcolini et al. (2006).

We first consider the explosion of a single SN Ia taking as initial values of the variables those obtained in the standard case at $t = 40$ Myr. The occurrence of the SN is mimicked by adding an extra amount $E_{\rm SN} = 10^{51}$ erg of thermal energy in the first three mesh points of the grid.

We point out that the binding energy of the gas at the moment of the explosion is only 44 per cent of that of the SN, so in principle the GC could be completely deprived of gas by the stellar explosion. However, given the large density of the gas itself, the radiative losses are rather effective, and in fact no gas is lost by the GC.

Fig. 6 shows the SNR expansion at three different times. As expected in a Sedov-like solution, a 'hole' is present behind the shock front. Contrary to a genuine Sedov solution, however, this hole is partially replenished by the FG high mass return rate that at this stage is nearly $8.9 \times 10^{-3}\,{\rm M}_\odot\,{\rm yr}^{-1}$. The gas replenishment

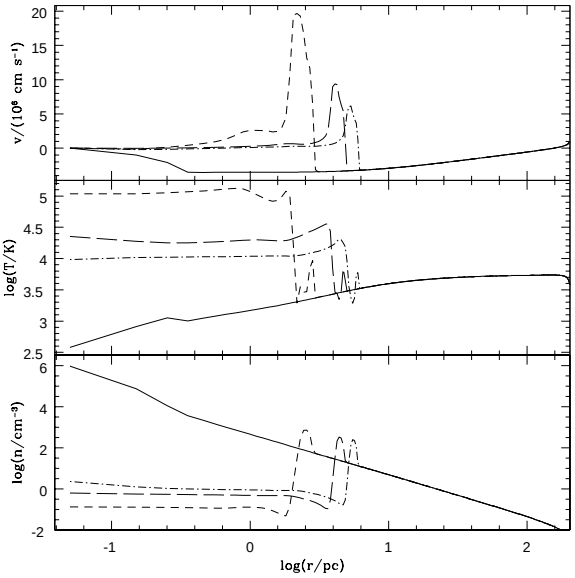

Figure 6. Velocity, temperature and density of the gas in the GC at $\Delta t = 10^4$ yr (dashed line), $\Delta t = 3 \times 10^4$ yr (long-dashed line) and $\Delta t = 5 \times 10^4$ yr (dot–dashed line) after a SN Ia explosion occurred in the standard model at $t = 40$ Myr. The solid lines show the radial profiles at $t = 40$ Myr just before the SN explosion. After $\Delta t = 5 \times 10^4$ yr another SN Ia is expected to explode (see text).

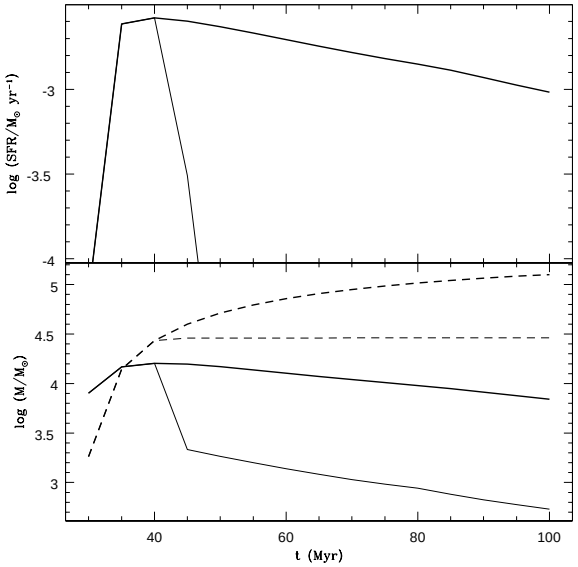

Figure 7. As Fig. 2, but for $M_{\rm FG} = 10^6\,{\rm M}_\odot$ and a flatter IMF (see text).

favours the radiative losses, thus weakening the SNR shock and slowing the remnant expansion below the escape velocity.

Although the effect of a single SN Ia explosion may therefore appear as a minor perturbation of the cooling flow, the cumulative effect of numerous SNe Ia drastically alters the gas dynamics. At $t = 40$ Myr the SN Ia rate is of the order of $2 \times 10^{-5}\,{\rm yr}^{-1}$ for $M_{\rm FG} = 10^7\,{\rm M}_\odot$ (Marcolini et al. 2006), i.e. one SN explosion every 5×10^4 yr (the maximum time-span considered in Fig. 6). More recent SNRs overlap older ones before these latter merge with the medium, and the sum of their actions has substantial consequences on the GC evolution. As shown in Fig. 2, the SFR quickly declines and the SG mass stops to grow attaining the value $M_{\rm SG} = 8.4 \times 10^4\,{\rm M}_\odot$. This result is obtained assuming a constant SN Ia rate up to 100 Myr; this assumption is largely justified as the actual rate suffers only a negligible reduction during this interval of time.

We point out that such a dramatic reduction of the SFR is due not only to a decrease in the gas content (the SFR being proportional to $\rho^{1.5}$), but also to the condition for star formation we have adopted (see equation 6). In fact, the gas is set into expansion over much of the GC volume by the SN explosions, and dynamical conditions are not favourable to further star formation.

In the end, as $M_{\rm SG}$ is only one-fifth of the value attained in the standard case, in order to obtain a cluster with a current total mass $M_{\rm now} \sim 1.7 \times 10^5\,{\rm M}_\odot$ with an equal amount of FG and SG stellar components, an initial FG population with $M_{\rm FG} = 10^7\,{\rm M}_\odot$ must lose ∼99 per cent of its mass.

It is interesting to note how differences in $M_{\rm FG}$ and/or the slope of the IMF influence the effectiveness of SNe in halting the formation of the SG stars. Fig. 5 shows that, contrary to the standard case, the flatter IMF essentially neutralizes the effect of the SNe Ia, as $M_{\rm SG}$ is only very slightly perturbed by the stellar explosions. In fact, when the SNe Ia start to explode the amount of gas is $M_{\rm g} = 7.6 \times 10^4\,{\rm M}_\odot$, a factor of 2.1 larger than in the standard case; as a consequence the radiative losses are roughly $2.1^2 = 4.2$ times greater, and suppress rather effectively any disruptive effect of the SNe.

Models with $M_{\rm FG} = 10^6\,{\rm M}_\odot$ show similar behaviour (see Figs 4 and 7), independent of the IMF adopted. In this case the gas has time to recover, at least in part, its inward convergent flow between successive SN explosions, because the SN Ia rate is 10 times lower than in the models with $M_{\rm FG} = 10^7\,{\rm M}_\odot$. Despite their lower rate, however, the stellar explosions are equally effective in reducing the gas in the cluster because of its lower binding energy in this case.

In principle, models in which the SF proceeds also during the SN activity would show today some stars polluted by the SN Ia ejecta. For example, let us examine the model with $M_{\rm FG} = 10^7\,{\rm M}_\odot$ and flatter IMF, which is the most favourable case to lock SN ejecta in SG stars, as illustrated in Fig. 5. The mass return rate at 40 Myr is $3.4 \times 10^{-2}\,{\rm M}_\odot\,{\rm yr}^{-1}$, while the mean production rate of metals by SNe Ia is $2.8 \times 10^{-5}\,{\rm M}_\odot\,{\rm yr}^{-1}$; as a consequence, the gas accumulating within the GC has a metallicity increment due to the SNe Ia $\Delta Z = 8.2 \times 10^{-4}$, which is comparable to the typical metallicity of GCs showing self-enrichment. On the other hand, star to star iron variations in GCs do not exceed ∼0.04 dex (Gratton et al. 2004), so that retention of SN Ia ejecta in SGs is ruled out by observations, with the exception of ω Cen (e.g. Marcolini et al. 2007).

4.5 Models with an extra energy source

In this section we explore the effect of an extra energy source due, for example, to X-ray binaries or a number of luminous hot planetary nebulae nuclei. In our model, this source is distributed as the FG stellar density and its total amount is equal to

$$Q = \int_0^{r_{\rm t}} 4\pi r^2 \rho_{\rm FG}(r) q \, {\rm d}r. \qquad (12)$$

We have carried out a number of exploratory simulations and found that, in general, a critical value $Q_{\rm cr}$ exists, separating models hosting a cooling flow from models hosting a wind. The transition between the two kinds of solutions happens rather abruptly as Q increases from values $Q < Q_{\rm cr}$ to values $Q > Q_{\rm cr}$. Such a sudden transition is due to the strong non-linearity of the radiative cooling term, which depends on the square of the gas density.

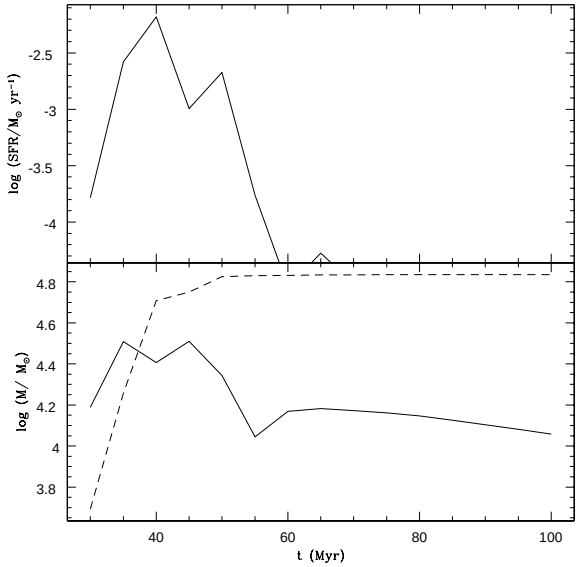

Figure 8. As Fig. 2, but with a diffuse energy source $Q = 6 \times 10^{37}$ erg s^{-1} included (see text).

Fig. 8 is analogous to Fig. 2 for a model similar to the standard one, but with $Q = Q_{\rm cr} = 6 \times 10^{37}$ erg s^{-1}. After an initial transient phase during which some SF occurs, a steady wind is established which prevents any further substantial growth of $M_{\rm SG}$. This case is borderline between a model with $Q = 4 \times 10^{37}$ erg s^{-1}, in which an almost normal star formation occurs, and one with $Q = 1.3 \times 10^{38}$ erg s^{-1}, where the immediate onset of a fast wind precludes any SG formation. For this set of models, the role of SNe Ia is negligible, as they start to explode when the SG star formation has already been halted. We stress that, for the standard model, we have $L_\sigma = 2 \times 10^{36}$ erg s^{-1} at $t = 28$ Myr, much lower than $Q_{\rm cr}$, as expected owing to the radiative losses (see Section 3.3).

We mention that $Q_{\rm cr} = 2 \times 10^{36}$ erg s^{-1} for the model with $M_{\rm FG} = 10^6$ M$_\odot$, while, for the models with flatter IMF, we have $Q_{\rm cr} = 6 \times 10^{38}$ and 2×10^{37} erg s^{-1} for $M_{\rm FG} = 10^7$ and 10^6 M$_\odot$, respectively. As expected, $Q_{\rm cr}$ is larger for flatter IMFs, because of the larger mass return rate which increases the radiative losses.

4.6 Models with different initial concentrations

In our standard model the FG is distributed following a King profile with concentration $c = \log(r_{\rm t}/r_{\rm c}) = 1.5$ (see Section 3). We analysed also cases with the same values of $M_{\rm FG}$ and $r_{\rm t}$ but different concentrations, namely $c = 0.75$, 1, 2 and 2.25. For these latter models, at $t = 28$ Myr one has $L_\sigma = 0.86 \times 10^{36}$, 1.1×10^{36}, 3.5×10^{36} and 5×10^{36} erg s^{-1}, respectively.

Within the range of values of c we have considered, the results are remarkably similar to those of the standard case, and in fact $Q_{\rm cr}$ varies only by a factor of $\sim$2, as shown in Fig. 9. There is a trend of increasing $Q_{\rm cr}$ with c due to the fact that the stellar density gets larger in the GC core; as a consequence, the gas density increases because of the larger mass return, and the radiative losses are stronger. A partial wind establishes in the outer regions, while a cooling flow persists in the core. Reverting such a 'mini-inflow' becomes increasingly more difficult for larger values of c. We point out that, although L_σ increases faster than the critical source, it remains always much lower than $Q_{\rm cr}$.

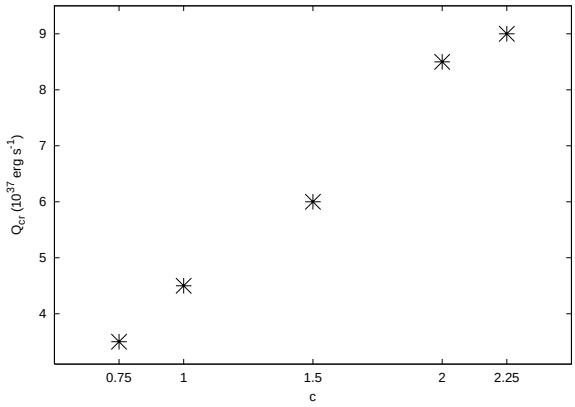

Figure 9. $Q_{\rm cr}$ as a function of the cluster concentration c for models with the same mass, IMF and truncation radius as the standard model.

4.7 Models with different initial truncation radii

In order to understand the influence of the assumed size of the FG population on the relative concentration of the SG stars, we ran models with the same mass $M_{\rm FG}$ and concentration c of the standard model, but with different values of the truncation radius ($r_{\rm t} = 40, 100, 400$ pc). The comparison among the models is summarized in Fig. 10 and shows only a minor dependence of the relative concentration of the two populations on the initial size of the cluster. In all cases the SG population is strongly concentrated in the cluster innermost regions, with 80–90 per cent of the total SG mass enclosed within $r/r_{\rm t} \sim 10^{-3}$–10^{-2}.

4.8 Consequences of the end of the cooling flow

The energy input either by recurrent SN Ia explosions or by distributed stationary sources with total power $> Q_{\rm cr}$ drastically limits

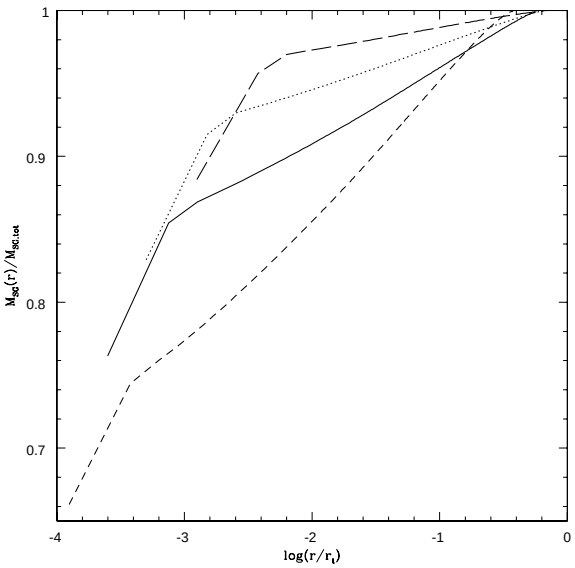

Figure 10. Radial profile of the SG stars at $t = 100$ Myr for models with $M_{\rm FG} = 10^7$ M$_\odot$, $c = 1.5$ and $r_{\rm t} = 40$ pc (long-dashed line), $r_{\rm t} = 100$ pc (dotted line), $r_{\rm t} = 200$ pc (solid line, standard model), $r_{\rm t} = 400$ pc (short-dashed line). The masses are normalized to their respective maximum values: $M_{\rm SG} = 4.8 \times 10^5$ M$_\odot$ (long-dashed line), $M_{\rm SG} = 4.8 \times 10^5$ M$_\odot$ (dotted line), $M_{\rm SG} = 4.45 \times 10^5$ M$_\odot$ (solid line, standard model), $M_{\rm SG} = 3.52 \times 10^5$ M$_\odot$ (short-dashed line).

the epoch of gas accretion and SG star formation in the cluster core. Clearly, there are a number of uncertain parameters in our understanding of SN Ia rates, and also their starting age and actual rate at early epochs may be smaller than we suggest (see Section 2.2).

Our simulations show that SN Ia explosions effectively clean clusters with initial masses in the range 10^6–$10^7\,M_\odot$ from AGB ejecta, and limit the SG formation time. We point out that this is no longer the case for more massive objects like the ultracompact dwarf galaxies, and possibly the progenitor of ω Cen, which are embedded in massive dark matter haloes, and which proceed to a more complex (but also more standard) chemical evolution (see Marcolini et al. 2006, 2007).

Concerning the stationary sources, $Q_{\rm cr} \sim 10^{38}\,{\rm erg\,s^{-1}}$ is of the order of the Eddington accretion luminosity for NSs, so a number of sub–Eddington accreting NSs distributed in the cluster could succeed in stopping the SG formation epoch. We know that several hundreds of NSs, revealed by their millisecond pulsar radio emission, are present in today's clusters (e.g. Heinke et al. 2005). Their radio emission (relevant for those NSs that are already spun up to millisecond periods at the early epoch we are considering) is in the plausible range 10^{34}–$10^{35}\,{\rm erg\,s^{-1}}$, so it has no global effect on the cooling flow. Only accreting NSs are good candidates as stationary source. Although only a few stationary X-ray sources are currently active in all the galactic GCs, the situation might have been different in the early stages of cluster evolution and this issue will need further investigation. As discussed in Section 2.2, NSs are just born from the highest mass super-AGBs, when the super-AGB winds are collecting in the core.

From the chemical point of view, the fact that the cooling flow is halted is important since it prevents less massive AGB stars from contributing to the formation of the SG. Although the maximum allowed age (and minimum allowed mass) strongly depends on the efficiency of convection, third dredge-up and mass loss in AGB stars, if the cooling flow is not halted and star formation prolongs beyond $\sim 10^8$ yr (the upper limit adopted in the standard hydro models of Section 4.1), in all the current stellar models the third dredge-up is important, and the yields are not compatible with the observed chemical anomalies; specifically, the total CNO abundances and the sodium abundance will be much larger than observed, and the oxygen abundance will not be reduced.

5 PRISTINE GAS

5.1 Motivations

If the SG formation time is too short, it will not meet the observational requirements, as not enough matter will be contained in the ejecta. One possible solution is the following: while the SN II events have wiped out the pristine matter from the cluster centre, during the AGB epoch it is possible that the pristine gas in the outskirts participates in the cooling flow. In the central regions it will mix with the AGB gas and contributes to star formation. In this way, the span of SF time required to achieve a massive SG is shorter. Further, the 'dilution' of the AGB ejecta by pristine gas may fully explain, in particular, the milder chemical anomalies (Prantzos & Charbonnel 2006; Decressin et al. 2007a,b; Ventura & D'Antona 2008a,b).

In all the models discussed in the previous sections, it has been assumed that the FG SNe II deprives the GC of all its pristine gas. In this section we drop this assumption and study a model in which part of the pristine gas contributes to the SG formation. We assume that initial asymmetries in the distribution of gas allow to vent out the SN II ejecta along preferential directions, creating an 'hourglass' cavity, and leaving part of the pristine gas in a substantially unperturbed torus at the outskirts of the cluster (e.g. Recchi, Matteucci & D'Ercole 2001).

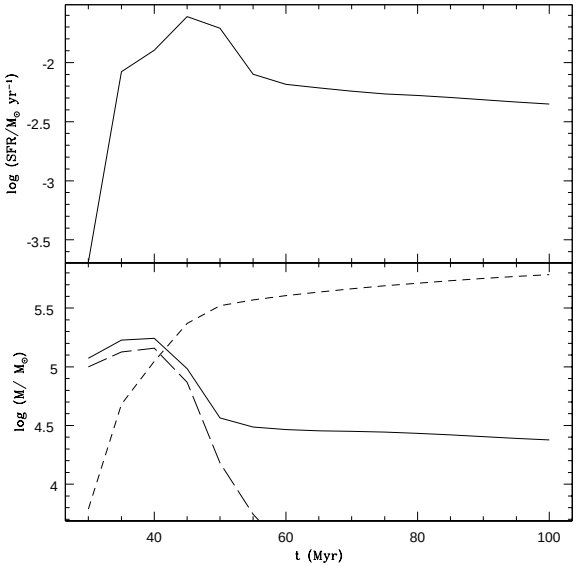

Figure 11. As Fig. 2, but for the infall model. The long-dashed line represents the amount of pristine gas.

5.2 Model with pristine gas infall

Since we use a 1D code for our hydrodynamical simulations, we cannot properly explore the case of SN II ejecta blown away through an axisymmetric chimney, with part of the pristine gas confined around it. We approximate this situation assuming an initial gas distribution within the GC with a central hole of radius $r = 150\,{\rm pc}$ and with a density radial profile $\rho(r) \propto r^{-2}$ beyond it. The total gas mass within the numerical grid is $M = 2.6 \times 10^5\,M_\odot$. These values are rather arbitrary, but nevertheless the model is useful to understand the consequences of the primordial gas infall on the SG formation process. All the other details of the model are the same as in the standard model.

As apparent in Fig. 11, after 100 Myr the total mass of SG stars formed, $M_{\rm SG} = 6.2 \times 10^5\,M_\odot$, is larger than that of the SG population formed in the standard model. This larger amount is created very quickly because part of the pristine gas is in place from the beginning and available for star formation. As this gas moves toward the centre, and more gas enters the GC from outside, the SFR increases. After $\sim$50 Myr no more pristine gas falls within the GC, and that already present has been locked within the SG stars formed till then (see the dashed line in the bottom panel of Fig. 11). As a consequence, the global evolution of the GC recovers its 'standard' behaviour (see Fig. 2).

Additional interesting details of this model are illustrated in Fig. 12, where the radial profiles of several quantities are displayed at two different times, namely $t = 40$ and 45 Myr. After 40 Myr the pristine gas has already largely moved toward the GC centre. However, the GC central volume included within $r \leq 10\,{\rm pc}$ still hosts only gas ejected by AGB stars, and the SG stars formed in this volume till this time have thus the same chemical characteristics of these polluters. Successively, up to $t \sim 50$ Myr (see Fig. 11), the pristine gas occupies all the GC volume and is well mixed with the

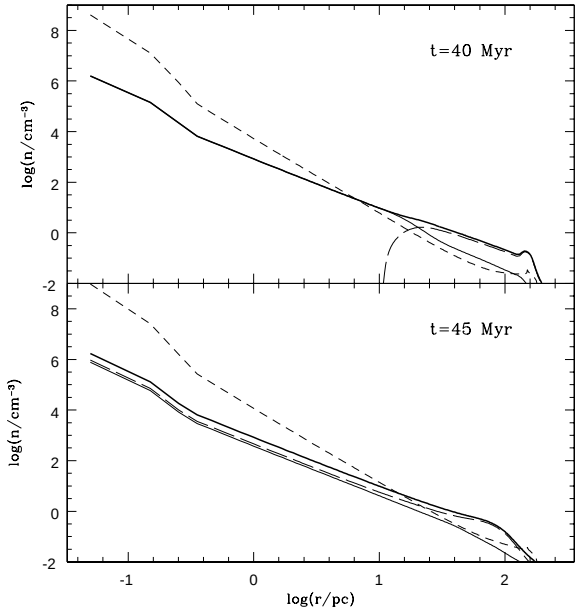

Figure 12. Radial profile of several quantities of the infall model at two different times: total gas density (thick solid line), pristine gas density (long-dashed line), AGB ejecta density (thin solid line), SG stellar density (dashed line).

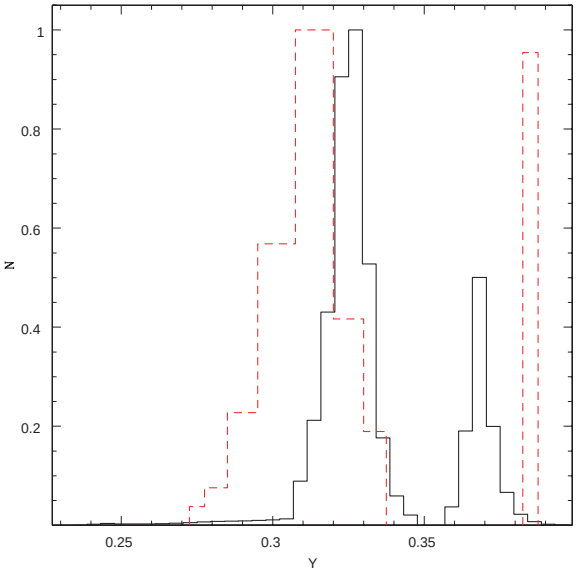

Figure 13. Histogram of the helium abundance of the SG stars formed in the model with the pristine gas infall (solid line). The dashed line shows the histogram of Y for NGC 2808 inferred by D'Antona & Caloi (2008) from the observations of the HB by Bedin et al. (2004) and from the MS distribution by Piotto et al. (2007). Each histogram is normalized to its maximum value.

gas returned by the FG stars. The stars forming in this period suffer a 'diluted' pollution. Finally, for $t > 50$ Myr, the FG stellar ejecta are again the only source of gas for the SG star formation and the chemical composition of the new SG stars formed after this time is that of the FG progenitors' ejecta.

At $t = 40$ Myr the SG stars formed at $r < 10$ pc have a mass $\sim 8.5 \times 10^4\,M_\odot$, and they are polluted by AGB stars with masses $M \geq 7\,M_\odot$ which are strong He polluters. For $40 < t < 50$ Myr the chemical contamination of the SG stars is diluted by the pristine gas all over the GC, and is due to FG stars with masses of 6–7 $M_\odot$.

5.3 Implications of the pristine gas infall for the very helium-rich population

Although the study of models including the infall of pristine gas will need to be extended and further explored, a number of interesting results have already emerged from the preliminary simulation discussed in the previous section.

We have shown that there is an epoch, between the end of SN II phase and the time when the pristine gas begins to mix with the super-AGB gas ejecta, during which, if the cluster is massive enough, the winds from the super-AGB stars are the only contributors to the cooling flow and the SG formation. We suggest that this is the phase during which the most extreme very helium-rich SG population can be formed. The super-AGBs can indeed have $Y \sim 0.38$ in their ejecta, and their gas will not be diluted. Thus a very homogeneous population with very high helium will be formed.

This early phase of very helium-rich SG star formation is followed by an epoch during which the pristine gas reaches the cluster inner regions and the SG stars form from gas in which the helium of the AGB ejecta, collected in the inner regions by the cooling flow, is diluted with the primordial helium. If the cooling flow goes on after the pristine gas is exhausted, stars will again be formed with undiluted ejecta, but the evolving AGB mass and its Y will be smaller (e.g. Pumo et al. 2008), giving rise to a 'helium gap' between the first very high helium stars and the other SG stars.

The scenario outlined here might lead to the formation of the blue MS in ω Cen and in NGC 2808, and of the extremely blue HB stars in other clusters (for a parametric approach to this problem, see Bekki et al. 2007).

We implemented in the code the helium abundance of the ejecta as a function of the initial stellar mass, following the Pumo et al. (2008) compilation, based on the AGB models by Ventura & D'Antona (2008a) and on the super-AGB models by Siess (2007a). Fig. 13 shows the predicted SG helium distribution for the infall model.

We see that a peak in the mass distribution is obtained at $Y \sim 0.37$, corresponding to the star formation in the cooling flow preceding the infall of pristine matter, and another, well distinct broader peak at medium He ($Y \sim 0.31$–0.34) is obtained from star formation when the wind matter is mixed with the pristine matter. There is a negligible tail of stars formed at $Y < 0.25$, so that this model implies that the 50 per cent stars having normal helium in NGC 2808 must indeed be a remnant of the FG population. In Fig. 13 we also show the Y distribution derived for the SG of the cluster NGC 2808 by D'Antona & Caloi (2008).

Although we have not made any attempt to find the initial parameters leading to the best fit of the observational Y distribution, the theoretical and the observed distribution are, in general, remarkably similar.

Since the helium yields from super-AGBs and AGBs are still uncertain, the amount of pristine matter involved, and its mixing with the FG matter is yet to be fully explored, we believe our results show that this scenario is a very promising step towards the understanding of the origin of the super He-rich population.

6 STELLAR DYNAMICAL EVOLUTION

One of the key requirements of the standard scenario presented in the previous sections is the large initial mass of the FG population. This

assumption, as we have discussed, is necessary for the formation of a significant SG population from the ejecta of intermediate-mass stars. The next issue to address in order to test the viability of the proposed scenario concerns the possible mechanisms driving the evolution of the ratio of the number of SG to FG stars.

Numerous studies of the dynamical evolution of star clusters (see e.g. Heggie & Hut 2003, and references therein for a review) have shown that internal two-body relaxation and tidal shocks cause stars to escape from clusters, eventually leading to complete cluster dissolution. With the exception of systems lying within a relatively narrow range of orbital parameters (see e.g. Vesperini & Heggie 1997), two-body relaxation is the dominant process driving the evaporation of stars from clusters. However, the two-body relaxation time-scale, $T_{\rm relax}$, increases with both the mass (M) and the size (R) of the system, $T_{\rm relax} \propto M^{1/2}R^{3/2}$ (see e.g. Heggie & Hut 2003). For a cluster with an initial mass of $10^7\,{\rm M}_\odot$, as adopted in the simulations presented in Section 4, the mass loss induced by internal two-body relaxation in one Hubble time is negligible. For example, the dissolution time predicted by N-body simulations (Baumgardt & Makino 2003) for a tidally limited cluster with initial mass $M = 10^7\,{\rm M}_\odot$, moving on a circular orbit at 4 kpc from the Galactic Centre, is about 480 Gyr. Hence two-body relaxation cannot be the process responsible for the loss a significant fraction of the initial FG population, or for the evolution of the ratio of the number of SG to FG stars.

A more promising mass reduction mechanism for the massive stellar systems considered in this study is the early mass loss associated with SN explosions in the FG population. In response to the loss of SN ejecta, a stellar system can expand beyond its tidal limit (Chernoff & Weinberg 1990; Fukushige & Heggie 1995), losing stars from its outer layers. The fraction of mass lost due to this expansion, and the implications for a cluster evolution, depend on the cluster structure, IMF and initial degree of mass segregation.

For initially unsegregated, tidally limited clusters with a Salpeter IMF, it has been shown that the mass loss resulting from this mechanism is negligible if the clusters are sufficiently centrally concentrated, with concentrations (as measured by the concentration parameter c defined earlier) similar to those typical ($1 \lesssim c \lesssim 2$; McLaughlin & van der Marel 2005) of Galactic GCs (Vesperini & Heggie 1997; Baumgardt & Makino 2003; McMillan & Portegies Zwart 2003). However, low-concentration clusters can lose a significant fraction of their mass in this way, and quickly dissolve (Chernoff & Shapiro 1987; Chernoff & Weinberg 1990; Fukushige & Heggie 1995; see also Vesperini & Zepf 2003 for the possible implications of this dissolution on populations of GCs).

Both the response of a cluster to this early mass loss and the critical concentration for its survival depend sensitively on the initial spatial distribution of massive stars. Several observational and theoretical studies (e.g. Hillenbrand 1997; Fischer et al. 1998; Hillenbrand & Hartmann 1998; Bonnell et al. 2001; de Grijs et al. 2002; Sirianni et al. 2002; Gouliermis et al. 2004; Stolte et al. 2006; McMillan, Vesperini & Portegies Zwart 2007) have suggested that clusters may form with a significant degree of initial mass segregation imprinted by the star formation process, or created dynamically very early in their evolution. As discussed in Vesperini, McMillan & Portegies Zwart (in preparation), initial mass segregation has dramatic implications for early cluster evolution. Specifically, in an initially segregated cluster, the mass lost due to SN explosions is preferentially removed from the innermost regions of the cluster, and can lead to rapid and significant overall expansion, mass loss and possibly dissolution, even for an initially highly concentrated system. Our N-body simulations do not include primordial gas; the effect of primordial gas expulsion would add to that of SN ejecta in triggering the cluster early expansion (see e.g. Boily & Kroupa 2003; Baumgardt & Kroupa 2007).

In the following sections we explore the role of this early expansion on the evolution of multiple population clusters and, in particular, its implications for the evolution of the cluster stellar populations relative abundance.

We begin with a general qualitative discussion of the scenario we have explored then illustrate the process using the results N-body simulations.

6.1 Cluster mass loss

In this section we outline the main elements of the dynamical mass-loss scenario, the processes and time-scales involved and the effect on the numbers of stars in the two populations.

The early evolution of the cluster is characterized by the rapid loss of FG stars. This is a consequence of cluster expansion in response to the dynamical heating from the loss of SN ejecta from the FG population: as the cluster expands beyond its tidal radius, the outer layers, which are predominantly populated by FG stars, are stripped. SG stars, which are mostly confined to the central regions, remain approximately constant in number during this phase. As a result, the number ratio of SG to FG stars increases rapidly. Hereafter, we will refer to the number ratio of long-lived SG to FG MS stars with masses in the range $0.1 < M/{\rm M}_\odot < 0.8$ as $f_{\rm MS}$.

The characteristic time-scale for this early evolution, expansion and stripping is the cluster dynamical time, $T_{\rm dyn} \propto M^{-1/2}\ R^{3/2}$, although the precise duration of this phase may range from $\sim$10 to $\sim 10^2$ dynamical times depending on the degree of initial mass segregation and the amount of impulsive mass loss; see e.g. fig. 3 in Vesperini et al. (2008).

The strength of this early expansion and the extent of the consequent loss of FG stars depend mainly on the degree of initial mass segregation, the amount of impulsive mass loss due SN and the structure of the cluster. As mentioned above, for clusters initially following a King density profile (King 1966) with concentrations similar to those currently observed in the Galactic GC system initial mass segregation plays a key role in triggering a strong expansion and early mass loss. As shown by Vesperini et al. (2008, in preparation) the heating due to a given amount of impulsive loss of SN ejecta is augmented by the preferential removal of the mass from the central regions.

A second important initial parameter is the ratio of the cluster 'King radius', $r_{\rm K}$, that is the limiting radius of the King model used to describe the system – to the cluster's tidal radius, $r_{\rm tidal}$, in the Galactic field: if $r_{\rm K}/r_{\rm tidal} < 1$, the cluster will not lose a significant number of stars until it fills its Roche lobe. For a cluster initially underfilling their Roche lobe, $f_{\rm MS}$ will start to evolve later and will eventually level off at a lower value than would be the case for a cluster with the same degree of initial mass segregation but initially filling the Roche lobe.

As the early expansion phase slows and eventually stops so do the loss rate of FG stars and the time evolution of $f_{\rm MS}$. The subsequent 'late' evolution is driven by two-body relaxation and proceeds on a time-scale, $T_{\rm relax}$, which is significantly longer than the dynamical time-scale. Two-body relaxation is responsible for mixing the SG and FG populations and for additional mass loss.

For the massive clusters of principal interest in this paper, the total mass loss due to two-body relaxation is small; for example, using the mass-loss rates derived from N-body simulations by Baumgardt

& Makino (2003) and the current observational values of mass and galactocentric distance, we estimate that a cluster like ω Cen should have lost at most about 5–10 per cent of its initial mass in one Hubble time by two-body relaxation.

The study of less massive multiple population clusters undergoing a significant relaxation driven mass loss will be the subject of a future paper. We note, however, that star loss induced by two-body relaxation affects all cluster regions and not just the stars in the outer layers as in the early phases of the cluster evolution. Both SG and FG stars escape as a result of two-body relaxation with the result that the variation of the relative abundance of the two populations is significantly smaller during this late relaxation-driven phase than during the early dynamical cluster expansion.

Although relaxation-driven stellar escape has a smaller effect on the relative abundance $f_{\rm MS}$ of the two populations, the evolution of this ratio may be affected by mixing, another process driven by two-body relaxation. The relevant time-scale in this case is the two-body relaxation time of the SG subsystem. As the low-mass SG stars evolve toward energy equipartition, the SG subsystem tends to expand, populating the outer regions of the cluster and mixing with FG stars. Once the two populations are mixed, even if the cluster is still undergoing a strong mass loss, the escaper population is no longer preferentially composed of FG stars and the number ratio of SG to FG stars stops increasing.

6.2 *N*-body simulations: initial conditions

We now present the results of *N*-body simulations aimed at quantitatively exploring the scenario outlined above.

We start our simulations with an initially segregated FG cluster of 25 000 stars. Mass segregation is set up by first letting the cluster evolve without including the effects of stellar evolution until the desired degree of segregation was reached by normal two-body relaxation. We emphasize that this is just the procedure used to generate a self-consistent initially segregated cluster model. It is not intended to model any stage of cluster evolution. The degree of initial segregation is such that the ratio of the initial half-mass radius of the entire system ($r_{\rm h}$) to the half-mass radius of stars more massive than $1\,{\rm M}_\odot$ ($r_{\rm h,1}$) is $r_{\rm h}/r_{\rm h,1} \simeq 1.5$.

Our model cluster is placed on a circular orbit at a galactocentric distance of $R_{\rm g} = 4\,{\rm kpc}$, with the Galactic tidal field modelled as a simple Keplerian potential of a point mass $M_{\rm g} \sim 4.3 \times 10^{10}\,{\rm M}_\odot$ (corresponding to a circular velocity $v_{\rm g} \sim 220\,{\rm km\,s^{-1}}$). We consider both a Roche lobe filing system ($r_{\rm K} = r_{\rm tidal}$), and three cases in which the system initially underfills its Roche lobe: $r_{\rm K}/r_{\rm tidal} = 0.75$, 0.6 and 0.5. Hereafter we refer to these simulations as SG-R1, SG-R075, SG-R06 and SG-R05, respectively.

SG stars are inserted into the simulation in a simplified way, by replacing, after about 30 Myr, the progenitor population of FG intermediate-mass stars ($4 < M/{\rm M}_\odot < 8$) by a SG population having masses between 0.1 and $0.8\,{\rm M}_\odot$ drawn from a Kroupa IMF. Following the results of the hydrodynamical simulations presented in Section 4, newborn SG stars are concentrated in the innermost regions of the cluster. In the *N*-body simulations, the SG stars are arbitrarily distributed according to a high-concentration $W_0 = 7$ ($c = 1.5$) King model, with a half-mass radius one-tenth of that of the initial FG system. The SG population is introduced with negligible velocity dispersion, and so undergoes an initial rapid phase of violent relaxation. Largely for this reason, the details of initial SG density distribution are unimportant in determining the subsequent evolution of the SG/FG system. The adopted initial density profiles of the two stellar populations are shown in Fig. 14.

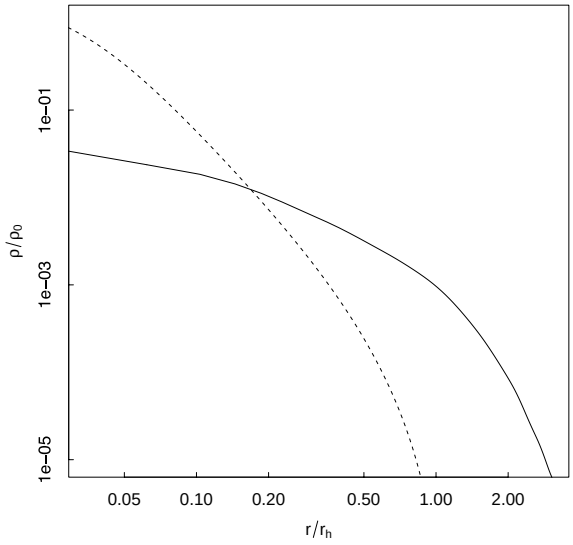

Figure 14. Initial density (normalized to the total central density ρ_0) profiles of FG (solid line) and SG (dashed line) stars.

As shown by analytical calculations and *N*-body simulations presented in Vesperini et al. (in preparation), the heating due to mass loss from (FG) SN ejecta increases both with the degree of initial mass segregation of the objects losing the mass and with the amount of impulsive mass loss. In order to clarify the implications of a lower level of initial mass segregation of the FG population and/or of a smaller amount of early impulsive mass loss from FG SN ejecta, we have repeated the SG-R1 simulation after decreasing the velocities of all FG stars so to reduce the initial virial ratio by approximately 10 and 30 per cent (changing directly the initial virial ratio of the system allows us to easily focus on and explore the effect of a different initial degree of mass segregation while leaving all the other cluster properties unchanged). Hereafter we refer to these two simulations as SG-C10 and SG-C30.

As described in the previous section, the scenario we are exploring is one in which cluster evolution is driven by multiple physical processes operating on different time-scales. For the massive systems of interest here, all the relevant time-scales (the dynamical time, the SG subsystem relaxation time and the cluster relaxation time) are significantly different from one another. In particular, the early dynamical evolution phase of the cluster is quite distinct from the later phase of relaxation-driven mixing and mass loss. In order to maintain this clear separation between the early and late evolutionary phases for the relatively small *N* system we can actually study, we have introduced into our *N*-body simulations a softening parameter equal to the average interparticle distance within the cluster half-mass radius in the calculation of the force. The effect of this softening is to increase the relaxation time-scale, avoiding the overlap between early rapid dynamical processes and late mixing and mass loss driven by two-body relaxation that would otherwise be found in the *N*-body models.

All simulations were carried out using the STARLAB package (Portegies Zwart et al. 2001, http://www.manybody.org/) accelerated by GRAPE-6 special-purpose hardware (Makino et al. 2003). STARLAB includes the effects of mass loss due to stellar evolution, two-body relaxation and the influence of the Galactic tidal field.

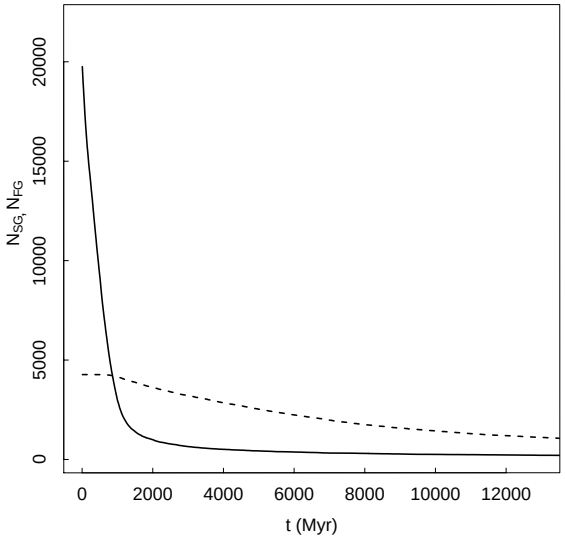

Figure 15. Time evolution of the number of SG (dashed line), FG (solid line) MS stars with $0.1 < M/\mathrm{M}_{\odot} < 0.8$ for the SG-R1 simulation.

6.3 *N*-body simulations: results

Fig. 15 shows the time evolution of the number of SG, $N_{\mathrm{SG,ms}}$, and FG, $N_{\mathrm{FG,ms}}$, MS stars with $0.1 < M/\mathrm{M}_{\odot} < 0.8$ for the SG-R1 simulation. The rapid preferential loss of FG stars during the cluster early evolution, discussed in Section 6.1, is clearly evident. As the cluster expands beyond its tidal radius in response to the loss of FG SN ejecta, its outer layers are stripped and a large fraction of the initial FG population is lost. The SG subsystem, on the other hand, is concentrated in the cluster inner regions and is largely unscathed by this early evolutionary process.

The early cluster expansion and associated mass loss slow significantly as the cluster gradually enters the phase driven by two-body relaxation. The time evolution of $f_{\mathrm{MS}} = N_{\mathrm{SG,ms}}/N_{\mathrm{FG,ms}}$ for all the models explored in our simulations is shown in Fig. 16. The early strong preferential loss of FG stars leads to a rapid increase of f_{MS}; subsequently when the cluster expansion and mass loss slow down, the growth rate of f_{MS} gradually decreases. Fig. 16 clearly illustrates the role of initial conditions in determining the current value of f_{MS} and suggests a possible origin for cluster-to-cluster variation in the relative abundance of different populations. Our simulations indicate that the typical observed values of $f_{\mathrm{MS}} \sim 0.5$–1.5 are attained by clusters initially underfilling their Roche lobe and/or with moderate levels of initial mass segregation.

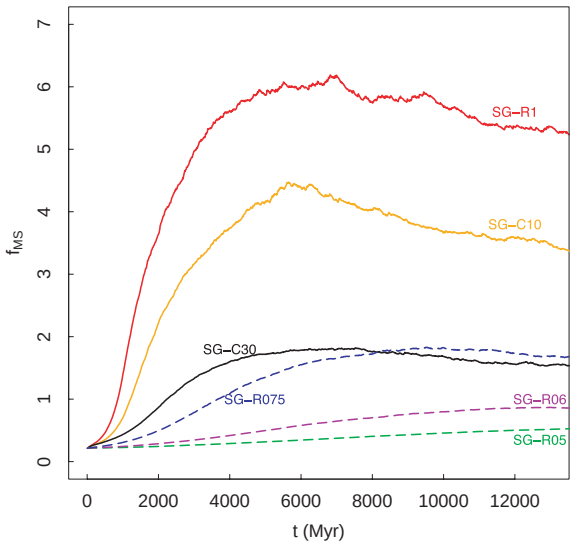

Figure 16. Time evolution of f_{MS}, the ratio of the number of SG to FG MS stars with $0.1 < M/\mathrm{M}_{\odot} < 0.8$, for all the *N*-body simulations presented in the paper.

Interestingly, our simulations also show possible evolutionary routes to the loss of most of the FG populations, leaving a cluster with a SG-dominated population. Initial conditions triggering the strong expansion necessary to strip most of the FG population are characterized by a larger degree of initial mass segregation and/or a larger amount of impulsive mass loss. The amount of impulsive mass loss will differ, for example, in clusters with the same stellar IMF and the same level of mass segregation but with different initial sizes (for example tidally truncated clusters at different galactocentric distances) and therefore different dynamical times. These clusters would lose the same amount of FG mass due to SN ejecta but for clusters with longer dynamical times, a larger fraction of this mass loss would occur in the impulsive regime, contributing to the heating that drives the cluster initial expansion.

As the structure and the abundances of the FG and SG populations evolve, the relative spatial distribution of the two populations also undergoes a significant variation.

Fig. 17 shows the evolution of the 10, 25, 50, 75 and 90 per cent Lagrangian radii for FG and SG MS stars with masses in the range $0.1 < M/\mathrm{M}_{\odot} < 0.8$ for the SG-R1 simulation (repeated in this case without softening in order to properly interpret the evolutionary time-scale in terms of the SG subsystem initial half-mass relaxation time).

Fig. 18 shows the radial profile of f_{MS} at three different times during the SG-R1 simulation. Our simulations predict that an initially strongly centrally peaked $f_{\mathrm{MS}}(r)$ profile will evolve toward a profile that is flat in the inner regions and decreasing in the outer parts. As the system evolves and the two populations continue to mix, the flat part of the profile (i.e. the region where the two populations have similar number density profiles) expands.

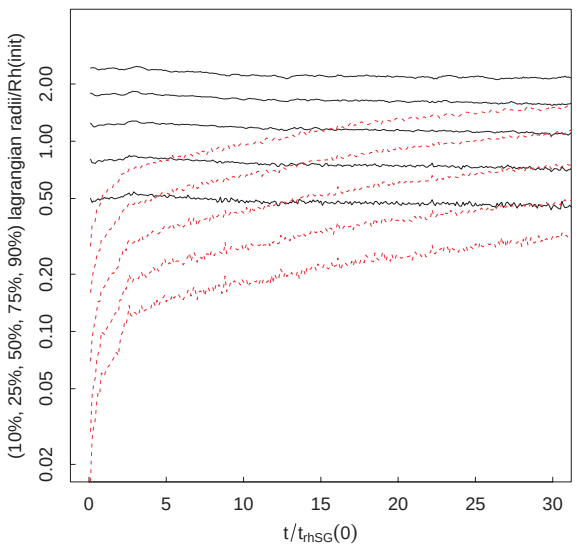

Figure 17. Time evolution of the 10, 25, 50, 75, 90 per cent Lagrangian radii of the FG (solid line) and the SG (dashed line) population of MS stars with $0.1 < M/\mathrm{M}_{\odot} < 0.8$ for the SG-R1 simulation. $t_{\mathrm{rh,\,SG}}(0)$ is the initial half-mass relaxation time of the SG subsystem.

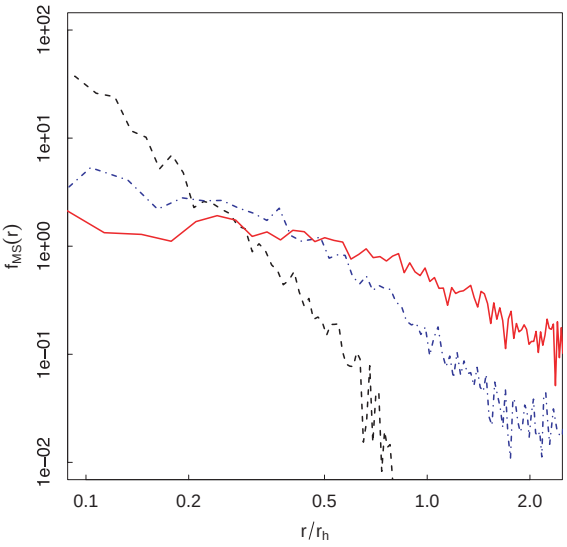

Figure 18. Radial profile of f_{MS} at $t/t_{rh,SG}(0) = 0, 10, 25$ (dashed black line, dot–dashed blue line, solid red line) for the SG-R1 simulation.

For a detailed comparison between the level of mixing in real clusters and that predicted by our simulations, we need an estimate of the ratio of the cluster age, T, to the initial SG subsystem half-mass relaxation time, $t_{rh,SG}(0)$. The lack of strong constraints on the initial conditions complicates such a comparison. However, if we plausibly adopt the current central relaxation time of ω Cen ($\sim$1 Gyr, see e.g. Harris 1996) as an estimate of the initial half-mass relaxation time of the SG subsystem, $T/t_{rh,SG}(0) \approx 10$. The radial profile of f_{MS} predicted by our simulations for this value of $T/t_{rh,SG}(0)$ is shown in Fig. 18. It is characterized by a central flat region where SG and FG stars are mixed, and declines in the outer cluster regions still dominated by FG MS stars.

We note that the presence of a declining outer part in the profile of $f_{MS}(r)$ is qualitatively consistent with the observed radial profile of the number ratio of blue to red MS stars in ω Cen (Sollima et al. 2007). Observations of the relative abundance of different populations in the inner regions of ω Cen and other multiple population clusters are needed to test the inner flattening predicted by our simulations. It is important to point out that while our predictions concerning the shape and evolution of the $f_{MS}(r)$ profile are general, the quantitative characteristics of this profile (e.g. the slope of the outer parts and the extension of the flat part of the profile) depend on several parameters including the initial relative concentration of the two populations, the details of their initial density profiles, the initial degree of mass segregation, the number of stars left in the cluster after the early mass loss and the cluster relaxation time. We therefore emphasize that a quantitative comparison between our theoretical $f_{MS}(r)$ profiles and observations must await the results of a more extended survey of simulations further exploring the space of initial parameters.

Our simulations show that both f_{MS} and the relative concentration of the two populations are significantly affected by dynamical evolution, and both depend on the cluster dynamical history and its initial conditions. We emphasize that the goal of the simulations reported here is to illustrate the key ingredients and dynamical processes behind the evolution of the relative number and spatial distribution of FG and SG stars. A more thorough survey of the parameters relevant to the scenario presented here is needed for a detailed comparison with observational data, and is currently in progress. The results will be presented elsewhere.

7 CONCLUSIONS

In this paper we have explored a scenario for the formation and the dynamical evolution of multiple stellar generations in GCs. A successful model for the origin and the evolution of clusters with multiple stellar generations needs to satisfy a number of observational constraints concerning the current chemical properties, relative abundance and structural properties of the different stellar populations.

After reviewing the main observational results on multiple population clusters, we have pointed out that the key issues to address concern the general origin of SG stars (among which those with very high helium content observed in the most massive clusters are only a fraction) and the identification of the evolutionary processes leading to clusters with a similar number of SG and FG stars (or even to clusters dominated by SG stars).

In order to address these different constraints and be able to model all the relevant aspects of multiple population clusters, we have combined the input from stellar evolution models to constrain the origin of the gas from which SG stars might form, hydrodynamical simulations to model the process of SG star formation and predict its initial structural properties and, finally, *N*-body simulations to explore the subsequent dynamical evolution of the two populations.

The main steps and results of this investigation are as follows.

7.1 Chemical abundances

We have reviewed all the issues concerning the super-AGB and massive AGB stars as the source of the polluted gas from which SG stars could form. The hypothesis that AGB stars might provide the gas for the SG formation has recently received some criticism in the literature based on possible inconsistencies between models and the observed chemical abundances in SG stars. However, in our review, we have pointed out that the results of chemical processing during the hot bottom burning phases are highly affected by the uncertainties in the basic input physics of these models, and that there is an ample range of plausible input parameters which can provide yields consistent with observations. In addition, recent models show that the super-AGB evolution can produce the helium content required for the very helium-rich population mentioned above. During the super-AGB epoch, between the end of SN II explosions and the beginning of the SN Ia explosions, there are no mechanisms preventing the formation of a cooling flow and the formations of the very helium-rich SG population from super-AGB winds.

7.2 Hydrodynamical simulations

We have carried out a number of hydrodynamical simulations to explore the dynamics of gas from super-AGB and AGB stellar winds and the process of formation of the SG population in the assumption that the SNe II belonging to the FG population clear the GC of its pristine gas.

(i) Our simulations show that this gas collects in a cooling flow into the innermost regions of the cluster where it forms SG stars. The cluster emerging from the hydrodynamical simulations is one with a SG strongly concentrated in the inner core of a more extended FG population. Initially the FG stars are the dominant stellar population with a total mass that must be about 10 times larger than the total

mass of the SG stars. The initial mass of the FG stars needs to be large enough to provide enough stellar mass return and form a substantial amount of SG stars.

(ii) We have explored the dependence of our results on the initial mass of the cluster, the stellar IMF and the initial cluster size and concentration. SG stars are always concentrated in the cluster innermost regions and the structure of the newly formed SG subsystem is largely independent of the cluster size and concentration.

(iii) Starting with a initial FG mass 10 times smaller than the value adopted in our standard model, leads to a SG total mass also 10 times smaller but does not alter the shape of the SG density profile or its concentration. For simulations with a flatter IMF the larger amount of gas supplied by AGB winds implies that a smaller star formation efficiency is needed to form the required mass of SG stars. If the requirement that the current mass of long-lived SG and FG stars are similar is maintained, a large FG initial mass is needed also for a flatter IMF. In this case the number of long-lived FG stars is smaller, and a large value of $M_{\rm FG}$ is still needed to have a current mass of long-lived FG stars consistent with observations.

(iv) The effects of SNe Ia and additional energy sources on the SG formation process have been investigated. Our simulations show that, for a 'normal' (e.g. Kroupa) IMF of the FG stars, the stellar explosions quickly evacuate most of the gas returned by the AGB stars, leading to a substantial drop in the gas content of the GC and to a suspension of the SG star formation. Given the uncertainties on the SN Ia rate, the interruption of the SF may occur in the time interval $40 < t < 100$ Myr. Flat IMFs produce an increment in the amount of returned gas, leading to an enhancement of the radiative losses and, possibly, to the inability of the SNe Ia to get rid of the gas. In this case SG stars continue to form and their chemical abundances should show the signature of the pollution by gas from SN ejecta. This however does not seem to be confirmed observationally and flat IMFs are thus disfavoured.

(v) We have further considered the possible presence of a diffuse energy source due to X-ray binaries and/or planetary nebulae. We show that for the standard model the cooling flow and the associated SG star formation can be halted by energy sources with a total power larger than 10^{38} erg s^{-1}.

(vi) We have also explored the possibility that the FG SNe II do not vent away all the pristine gas, and that part of it remains gravitationally bound to the cluster and falls back on to it after an initial ousting. The SG stars forming in the cluster central regions before this pristine gas reaches the cluster core originate from pure ejecta of the super-AGB stars which is very helium rich. These stars may form the very helium-rich population present in the most massive GCs. Once the pristine gas has fallen back in the cluster, SG stars form in an ambient medium in which the helium abundance is 'diluted', and give rise to the moderately helium-rich population.

7.3 Stellar dynamical simulations

The subsequent dynamical evolution of the cluster has been studied by means of *N*-body simulations.

(i) One of the critical issues for viability of the scenario presented here is the identification of a mechanism leading to the escape of a large fraction of the initial FG population. For clusters as massive as required by our hydrodynamical models, the mass lost in one Hubble time due to two-body relaxation is negligible.

Following observational and theoretical studies suggesting that initial mass segregation may be imprinted in clusters by the star formation process or produced dynamically early in the cluster evolution, we have studied the evolution of initially segregated clusters. In our simulations, a large fraction of FG cluster stars is lost early in the cluster evolution due to the expansion and stripping of the cluster outer layers resulting from early mass loss associated with FG SN ejecta. Initial FG mass segregation plays a key role since the heating and the expansion due to the loss of SN ejecta are augmented by the preferential removal of the mass from the inner regions of the cluster.

(ii) The population of escapers is dominated by FG stars. The SG population, initially concentrated in the innermost cluster regions, is largely unscathed by the early mass loss. We find that the early cluster evolution and mass loss can lead to a significant loss of FG stars and to current values of $f_{\rm MS}$, consistent with observations ($0.5 < f_{\rm MS} < 1.5$). We have also demonstrated possible evolutionary routes leading to the loss of most of the FG population and leaving a SG-dominated cluster. Clusters initially filling their Roche lobe with higher degrees of initial mass segregation and/or losing impulsively a larger fraction of SN ejecta undergo more expansion and may lose most of their FG stars.

(iii) After the initial phase of expansion and mass loss, cluster evolution is driven by two-body relaxation which results in the spatial mixing of the two populations. Following the hydrodynamical simulations, in the *N*-body initial conditions SG stars are concentrated in the inner regions of the cluster. The radial profile of the number ratio of SG to FG stars, $f_{\rm MS}(r)$, is initially a decreasing function of radius. We find that, as the cluster evolves and the two populations mix, $f_{\rm MS}(r)$ flattens in the inner parts of the cluster. The central flat region of the $f_{\rm MS}(r)$ radial profile expands on a relaxation time-scale as mixing proceeds. In general, unless mixing is complete, we predict that $f_{\rm MS}(r)$ is characterized by a flat inner part and a declining portion in the outer regions of the cluster.

A more extended survey of hydrodynamical and *N*-body simulations to further explore the dynamics and the implications of the scenario presented here as well as for a more detailed comparison with observations is currently in progress and will be presented in future papers.

ACKNOWLEDGMENTS

We thank Luca Ciotti for useful discussions. AD, FD and SR were supported in part by INAF under PRIN 2005 'Experimenting stellar nucleosynthesis in clean environments'. EV and SLWM were supported in part by NASA grants NNX07AG95G and NNX08AH15G, and by NSF grant AST-0708299.

REFERENCES

Baumgardt H., Kroupa P., 2007, MNRAS, 380, 1589
Baumgardt H., Makino J., 2003, MNRAS, 340, 227
Bedin L. R., Piotto G., Anderson J., Cassisi S., King I. R., Momany Y., Carraro G., 2004, ApJ, 605, L125
Bedogni R., D'Ercole A., 1986, A&A, 157, 101
Bekki K., Norris J. E., 2006, ApJ, 637, L109
Bekki K., Campbell S. W., Lattanzio J. C., Norris J. E., 2007, MNRAS, 377, 335
Boily C., Kroupa P., 2003, MNRAS, 338, 673
Bonnell I. A., Clarke C. J., Bate M. R., Pringle J. E., 2001, MNRAS, 324, 573
Busso G. et al., 2007, A&A, 474, 105
Caloi V., D'Antona F., 2005, A&A, 435, 987
Caloi V., D'Antona F., 2007, A&A, 463, 949
Cameron A. G. W., Fowler W. A., 1971, ApJ, 164, 111
Canuto V. M., Goldman I., Mazzitelli I., 1996, ApJ, 473, 550

Carretta E., Bragaglia A., 2008 in Proc. MPA/ESO/MPE/USM Joint Astron. Conf., Chemical Evolution of Dwarf Galaxies and Stellar Clusters
Carretta E., Gratton R. G., Lucatello S., Bragaglia A., Bonifacio P., 2005, A&A, 433, 597
Carretta E., Bragaglia A., Gratton R. G., Leone F., Recio-Blanco A., Lucatello S., 2006, A&A, 450, 523
Carretta E., Recio-Blanco A., Gratton R. G., Piotto G., Bragaglia A., 2007, ApJ, 671, L125
Cassisi S., Salaris M., Pietrinferni A., Piotto G., Milone A. P., Bedin L. R., Anderson J., 2008, ApJ, 672, L115
Chernoff D. F., Shapiro S. L., 1987, ApJ, 322, 113
Chernoff D. F., Weinberg M. D., 1990, ApJ, 351, 121
Choi E., Yi S. K., 2008, MNRAS, 386, 1332
Ciotti L., D'Ercole A., Pellegrini S., Renzini A., 1991, ApJ, 376, 380
Cohen J. G., Meléndez J., 2005, AJ, 129, 303
Cohen J. G., Briley M. M., Stetson P. B., 2002, AJ, 123, 2525
Cohen J. G., Briley M. M., Stetson P. B., 2005, AJ, 130, 1177
Cottrell P. L., Da Costa G. S., 1981, ApJ, 245, L79
D'Antona F., Caloi V., 2004, ApJ, 611, 871
D'Antona F., Caloi V., 2008, MNRAS, 390, 693
D'Antona F., Caloi V., Montalbán J., Ventura P., Gratton R., 2002, A&A, 395, 69
D'Antona F., Bellazzini M., Caloi V., Pecci F. F., Galleti S., Rood R. T., 2005, ApJ, 631, 868
D'Antona F., Ventura P., Caloi V., 2007, in Vallenari A., Tantalo R., Portinari L., Moretti A., eds, ASP Conf. Ser. Vol. 374, From Stars to Galaxies: Building the Pieces to Build Up the Universe. Astron. Soc. Pac., San Francisco, p. 155
Decressin T., Meynet G., Charbonnel C., Prantzos N., Ekström S., 2007a, A&A, 464, 1029
Decressin T., Charbonnel C., Meynet G., 2007b, A&A, 475, 859
de Grijs R., Gilmore G. F., Johnson R. A., Mackey A. D., 2002, MNRAS, 331, 245
Dessart L., Burrows A., Ott C. D., Livne E., Yoon S.-C., Langer N., 2006, ApJ, 644, 1063
Downing J. M. B., Sills A., 2007, ApJ, 662, 341
Fenner Y., Campbell S., Karakas A. I., Lattanzio J. C., Gibson B. K., 2004, MNRAS, 353, 789
Fischer P., Pryor C., Murray S., Mateo M., Richtler T., 1998, AJ, 331, 592
Fukushige T., Heggie D. C., 1995, MNRAS, 276, 206
Gouliermis D., Keller S. C., Kontizas M., Kontizas E., Bellas-Velidis I., 2004, A&A, 416, 137
Gratton R., Sneden C., Carretta E., 2004, ARA&A, 42, 385
Harris W. E., 1996, AJ, 112, 1487
Heggie D., Hut P., 2003, The Gravitational Million-Body Problem. Cambridge Univ. Press, Cambridge
Heinke C. O., Grindlay J. E., Edmonds P. D., Cohn H. N., Lugger P. M., Camilo F., Bogdanov S., Freire P. C., 2005, in Burderi L. et al., eds, AIP Conf. Proc. 797, Interacting Binaries: Accretion, Evolution, and Outcomes. Am. Inst. Phys., New York, p. 40
Hillenbrand L. A., 1997, AJ, 113, 1733
Hillenbrand L. A., Hartmann L. W., 1998, ApJ, 492, 540
Hunter I. et al., 2008, ApJ, 676, L29
Iben I., Jr, 1985, QJRAS, 26, 1
Iben I., Jr, Renzini A., 1983, ARA&A, 21, 271
Iben I. J., Ritossa C., Garcia-Berro E., 1997, ApJ, 489, 772
Ivanova N., Heinke C. O., Rasio F. A., Belczynski K., Fregeau J. M., 2008, MNRAS, 386, 553
Karakas A., Lattanzio J. C., 2007, Publ. Astron. Soc. Aust., 24, 103
Karakas A. I., Fenner Y., Sills A., Campbell S. W., Lattanzio J. C., 2006, ApJ, 652, 1240
King I. R., 1966, AJ, 71, 64
King I. R., Anderson J., Cool A. M., Piotto G., 1998, ApJ, 492, L37
Kraft R. P., 1994, PASP, 106, 553
Kroupa P., Tout C. A., Gilmore G., 1993, MNRAS, 262, 545
Lee Y.-W. et al., 2005, ApJ, 621, L57
Li Y., Burstein D., 2003, ApJ, 598, L103
McLaughlin D. E., van der Marel R. P., 2005, ApJS, 161, 304
McMillan S., Portegies Zwart S., 2003, ApJ, 596, 314
McMillan S. L. W., Vesperini E., Portegies Zwart S. F., 2007, ApJ, 655, L45
Maeder A., Meynet G., 2006, A&A, 448, L37
Makino J., Fukushige T., Koga M., Namura K., 2003, PASJ, 55, 1163
Mannucci F., Della Valle M., Panagia N., 2006, MNRAS, 370, 773
Marcolini A., D'Ercole A., Brighenti F., Recchi S., 2006, MNRAS, 371, 643
Marcolini A., Sollima A., D'Ercole A., Gibson B. K., Ferraro F. R., 2007, MNRAS, 382, 443
Marshall J. R., van Loon J. T., Matsuura M., Wood P. R., Zijlstra A. A., Whitelock P. A., 2004, MNRAS, 355, 1348
Mathews W. G., Brighenti F., 1999, ApJ, 526, 114
Matteucci F., Recchi S., 2001, ApJ, 558, 351
Milone A. P. et al., 2008, ApJ, 673, 241
Nomoto K., 1984, ApJ, 277, 791
Norris J. E., 2004, ApJ, 612, L25
Paczyński B., 1971, Acta Astron., 21, 271
Padovani P., Matteucci F., 1993, ApJ, 416, 26
Piotto G. et al., 2005, ApJ, 621, 777
Piotto G. et al., 2007, ApJ, 661, L53
Poelarends A. J. T., Herwig F., Langer N., Heger A., 2008, ApJ, 675, 614
Portegies Zwart S. F., McMillan S. L. W., Hut P., Makino J., 2001, MNRAS, 321, 199
Prantzos N., Charbonnel C., 2006, A&A, 458, 135
Pumo M. L., D'Antona F., Ventura P., 2008, ApJ, 672, L25
Recchi S., Matteucci F., D'Ercole A., 2001, MNRAS, 322, 800
Rich R. M. et al., 1997, ApJ, 484, L25
Richer H. B. et al., 2006, Sci, 313, 936
Ritossa C., García-Berro E., Iben I. J., 1999, ApJ, 515, 381
Romano D., Matteucci F., Tosi M., Pancino E., Bellazzini M., Ferraro F. R., Limongi M., Sollima A., 2007, MNRAS, 376, 405
Rosen A., Bregman J. N., 1995, ApJ, 440, 634
Sackmann I. J., Boothroyd A. I., 1992, ApJ, 392, L71
Salaris M., Weiss A., Ferguson J. W., Fusilier D. J., 2006, ApJ, 645, 1131
Siess L., 2006, A&A, 448, 717
Siess L., 2007a, A&A, 476, 893
Siess L., 2007b, in Kerschbaum F., Charbonnel C., Wing R. F., eds, ASP Conf. Ser. Vol. 378, Why Galaxies Care About AGB Stars: Their Importance as Actors and Probes. Astron. Soc. Pac., San Francisco, p. 9
Sirianni M., Nota A., De Marchi G., Leitherer C., Clampin M., 2002, ApJ, 579, 275
Sneden C., Kraft R. P., Guhathakurta P., Peterson R. C., Fulbright J. P., 2004, AJ, 127, 2162
Sollima A., Ferraro F. R., Bellazzini M., Origlia L., Straniero O., Pancino E., 2007, ApJ, 654, 915
Stanford L. M., Da Costa G. S., Norris J. E., Cannon R. D., 2006, ApJ, 647, 1075
Stolte A., Brandner W., Brandl B., Zinnecker H., 2006, AJ, 132, 253
Van Winckel H., 2003, ARA&A, 41, 391
Ventura P., D'Antona F., 2005a, A&A, 431, 279
Ventura P., D'Antona F., 2005b, A&A, 439, 1075
Ventura P., D'Antona F., 2008a, A&A, 479, 805
Ventura P., D'Antona F., 2008b, MNRAS, 385, 2034
Ventura P., D'Antona F., Mazzitelli I., Gratton R., 2001, ApJ, 550, L65
Vesperini E., Heggie D. C., 1997, MNRAS, 289, 898
Vesperini E., Zepf S. E., 2003, ApJ, 587, L97
Vesperini E., McMillan S. L. W., Portegies Zwart S. F., 2008, in Vesperini E., Giersz M., Sills A., eds, Proc. IAU Symp. 246, Dynamical Evolution of Dense Stellar Systems. Cambridge Univ. Press, Cambridge, p. 181
Villanova S. et al., 2007, ApJ, 663, 296
Yong D., Grundahl F., 2008, ApJ, 672, L29
Yoon S.-J., Joo S.-J., Ree C. H., Han S.-I., Kim D.-G., Lee Y.-W., 2008, ApJ, 677, 1080

APPENDIX A

The result of our simulations proved to be essentially independent of the value of ν. To understand why, let us consider a one-zone toy model in which the gas density ρ and the stellar density ρ_* evolve following the two equations:

$$\frac{\mathrm{d}\rho}{\mathrm{d}t} = -\nu\rho^2 + s, \tag{A1}$$

$$\frac{\mathrm{d}\rho_*}{\mathrm{d}t} = \nu\rho^2. \tag{A2}$$

The constant ν regulates the SF efficiency and the constant s is a source term representing the rate at which the gas is replenished. The SF time-scale $t_{\rm sf} = 1/\nu\rho$ depends on the gas density as the cooling time rather than the free-fall time, which instead is the actual time-scale encountered in our simulations. With the present definition, however, it is possible to obtain an analytical solution to the above equations without invalidating our main conclusions (see Section 3.2). The solution of equation (A1) is

$$\rho(t) = \left(\frac{s}{\nu}\right)^{0.5} \tanh\left(\frac{t}{\tau}\right), \tag{A3}$$

where $\tau = (\nu\ s)^{-0.5}$. Then the solution of equation (A2) is

$$\rho_*(t) = \left(\frac{s}{\nu}\right)^{0.5} \left[\left(\frac{t}{\tau}\right) - \tanh\left(\frac{t}{\tau}\right)\right]. \tag{A4}$$

Defining the replenishing time-scale as $t_{\rm rp} = \rho/s$, one obtains $\tau = (t_{\rm sf}t_{\rm rp})^{0.5}$. In words, the growth time-scale of the stars is given by the geometric mean of the SF and replenishing time-scales, and is therefore of the same order of magnitude. This time-scale is necessarily much shorter than the evolution time of the system over which equations (A1) and (A2) are solved. In fact, these equations are meaningless for $t/\tau < 1$ because neither appreciable SF nor significant stellar mass loss can occur during a time interval that short. In the meaningful case in which $t/\tau \gg 1$, equation (A4) becomes

$$\rho_*(t) = st. \tag{A5}$$

The growth of the stellar population is thus independent of ν and depends on the replenishing rate, a result confirmed by our simulations.

This paper has been typeset from a TEX/LATEX file prepared by the author.